

Mass-dependent fractionation of quadruple stable sulfur isotope system as a new tracer of sulfur biogeochemical cycles

Shuhei Ono ^{a,*}, Boswell Wing ^b, David Johnston ^b, James Farquhar ^b, Douglas Rumble ^a

^a *Geophysical Laboratory, Carnegie Institution of Washington, 5251 Broad Branch Rd. NW, Washington, DC 20015, USA*

^b *Department of Geology and Earth System Science Interdisciplinary Center, University of Maryland, College Park, MD 20742, USA*

Received 4 April 2005; accepted in revised form 18 January 2006

Abstract

Sulfur isotope studies of post-Archean terrestrial materials have focused on the ratio $^{34}\text{S}/^{32}\text{S}$ because additional isotopes, ^{33}S and ^{36}S , were thought to carry little information beyond the well-known mass-dependent relationship among multiple-isotope ratios. We report high-precision analyses of $\Delta^{33}\text{S}$ and $\Delta^{36}\text{S}$ values, defined as deviations of ^{33}S and ^{36}S from ideal mass-dependent relationships, for international reference materials and sedimentary sulfides of Phanerozoic age by using a fluorination technique with a dual-inlet isotope ratio mass spectrometer. Measured variations in $\Delta^{33}\text{S}$ and $\Delta^{36}\text{S}$ are explained as resulting from processes involve branching reactions (two or more reservoirs formed) or mixing. Irreversible processes in closed systems (Rayleigh distillation) amplify the isotope effect. We outline how this new isotope proxy can be used to gain new insights into fundamental aspects of the sulfur biogeochemical cycle, including additional constraints on seawater sulfate budget and processes in sedimentary sulfide formation. The isotope systematics discussed here cannot explain the much larger variation of $\Delta^{33}\text{S}$ and $\Delta^{36}\text{S}$ observed in Archean rock records. Furthermore, Phanerozoic samples we have studied show a characteristic $\Delta^{33}\text{S}$ and $\Delta^{36}\text{S}$ relationship that differs from those measured in Archean rocks and laboratory photolysis experiments. Thus, high precision analysis of $\Delta^{33}\text{S}$ and $\Delta^{36}\text{S}$ can be used to distinguish small non-zero $\Delta^{33}\text{S}$ and $\Delta^{36}\text{S}$ produced by mass-dependent processes from those produced by mass-independent processes in Archean rocks and extraterrestrial materials.

© 2006 Elsevier Inc. All rights reserved.

1. Introduction

Sulfur (^{32}S , ^{33}S , ^{34}S , and ^{36}S) and oxygen (^{16}O , ^{17}O , and ^{18}O) have more than two stable isotopes. Until recently, however, interest in measuring more than one isotope ratio was limited to researchers who study extraterrestrial materials (Hulston and Thode, 1965b; Clayton et al., 1973). This is because isotope discriminations in terrestrial processes follow mass-dependent relationships (i.e., $\delta^{17}\text{O} \approx 0.52 \delta^{18}\text{O}$, $\delta^{33}\text{S} \approx 0.52 \delta^{34}\text{S}$, and $\delta^{36}\text{S} \approx 1.9 \delta^{34}\text{S}$) such that additional isotope ratios (i.e., $^{17}\text{O}/^{16}\text{O}$, $^{33}\text{S}/^{32}\text{S}$, and $^{36}\text{S}/^{32}\text{S}$) were thought to carry little or no additional information. One reason for increased interests in measuring rare isotopes for Earth materials was the discovery of anomalous ^{17}O abundance in a wide variety of atmospheric

trace gases (Schueler et al., 1990; Thiemens, 1999; Brenninkmeijer et al., 2003) as a result of mass-independent fractionation in the ozone recombination reaction (Thiemens and Heidenreich, 1983; Mauersberger et al., 1999; Gao and Marcus, 2001). Recent multiple-sulfur isotope studies have been fueled by a discovery of anomalous ^{33}S and ^{36}S abundances in Archean sulfate and sulfide minerals that reflect unique atmospheric sulfur chemistry in an early anoxic atmosphere (Farquhar et al., 2000a; Ono et al., 2003; Mojzsis et al., 2003).

Bender et al. (1994) suggested atmospheric O_2 might carry mass-independent components that might result as a mass-independent depletion of ^{17}O (of $\sim 0.2\%$). This has important implication to the global atmospheric O_2 cycle because the signature can be used to determine relative rates for production of mass-independent anomaly in stratospheric chemistry and destruction by mass-dependent fractionation in biological photosynthesis and respiration

* Corresponding author. Fax: +1 202 478 8901.

E-mail address: s.ono@gl.ciw.edu (S. Ono).

(Luz et al., 1999; Luz and Barkan, 2000; Blunier et al., 2002). Young et al. (2002), however, pointed out that different mass-dependent relationships (i.e., $^{17}\theta = \ln(^{17}\alpha)/\ln(^{18}\alpha)$) for different processes might explain observed ^{17}O depletion without introducing stratospheric mass-independent contribution. Recent studies, thus, focused on the accurate characterization of $^{17}\theta$ values for respiratory processes (Angert et al., 2003; Luz and Barkan, 2005) and hydrological cycle and plant evapotranspiration (Angert et al., 2004).

Work with sulfur isotopes (Farquhar et al., 2003) has also reported that isotope effect associated with a biological sulfate reduction is characterized by $^{33}\theta$ ($= \ln(^{33}\alpha)/\ln(^{34}\alpha)$) that is different from the value expected from equilibrium isotope fractionation. It was suggested that the multiple-sulfur isotope system can be used to study biosynthetic pathways of microbial sulfate reduction and sulfur dispropotionation network (Farquhar et al., 2003; Johnston et al., 2005). These studies also provide a way to identify the signatures of different sulfur metabolisms, even when $\delta^{34}\text{S}$ fractionations are identical.

In this paper, we will investigate multiple-sulfur isotope systematics in mass-dependent processes operating in natural environments. We will (1) describe the origin of small magnitude $\Delta^{33}\text{S}$ and $\Delta^{36}\text{S}$ values in mass-dependent processes, (2) demonstrate that these new isotope proxies are measurable by a fluorination technique coupled with dual-inlet gas-source mass-spectrometry, (3) report results of quadruple sulfur isotope analyses of sedimentary biogenic pyrite, and (4) develop mathematical models to describe how we can use this new isotope proxy to gain new insights into processes of sedimentary sulfide formation and global sulfur budgets. The multiple sulfur isotope systematics discussed here are also applicable for any isotope system that has more than two isotopes. Such applications for geological materials, however, may be limited by the precision of the analytical techniques (see, Sessions and Hayes, 2005 for brief discussion about triple hydrogen isotope system, H/D/T).

2. Definitions and systematics of $\Delta^{33}\text{S}$ and $\Delta^{36}\text{S}$

2.1. Definitions of $\Delta^{33}\text{S}$ and $\Delta^{36}\text{S}$

Several recent papers discuss definitions for $\Delta^{17}\text{O}$ (Miller, 2002; Young et al., 2002; Kaiser et al., 2004; Assonov and Brenninkmeijer, 2005) and $\Delta^{33}\text{S}$ (Farquhar et al., 2000c; Ono et al., 2003). Each definition has certain advantages and disadvantages to the others in terms of normalization and applications in natural systems. Here, we describe the definitions we use in this paper, and briefly discuss the systematics that apply to natural processes.

Sulfur isotopic compositions are reported using conventional delta notation

$$\delta^x\text{S} = \left(\frac{{}^xR_{\text{sample}}}{{}^xR_{\text{reference}}} - 1 \right) \times 1000 \text{ (‰)}, \quad (1)$$

where xR are the isotope ratios (${}^x\text{S}/^{32}\text{S}$, where $x = 33, 34, 36$) of sample and reference materials. In this study, we also use modified delta values (Hulston and Thode, 1965b; Young et al., 2002; Angert et al., 2004)

$$\delta^x\text{S}' = \ln \left(\frac{{}^xR_{\text{sample}}}{{}^xR_{\text{reference}}} \right) \times 1000 \text{ (‰)}. \quad (2)$$

The two delta scales are related by

$$\delta^x\text{S}' = \ln \left(\frac{\delta^x\text{S}}{1000} + 1 \right) \times 1000 \text{ (‰)}. \quad (3)$$

Some researchers used $\ln(1 + \delta^x\text{O})$ notation in place of $\delta^x\text{O}'$ notation by omitting scaling factor of 1000 in Eq. (3) (e.g., Kaiser et al., 2004; Assonov and Brenninkmeijer, 2005; Luz and Barkan, 2005). As we will see in the later section, the $\delta^x\text{S}'$ notation simplifies some mathematical treatments. In this paper, however, we report $^{34}\text{S}/^{32}\text{S}$ ratios in $\delta^{34}\text{S}$ scale to be compatible with existing literatures on sulfur isotope geochemistry.

A power law has been used to describe mass-dependent isotope fractionation (Hulston and Thode, 1965b; Miller, 2002; Young et al., 2002):

$${}^{33}\alpha_{\text{A/B}} = {}^{34}\alpha_{\text{A/B}}^{33\theta} \quad \text{and} \quad {}^{36}\alpha_{\text{A/B}} = {}^{34}\alpha_{\text{A/B}}^{36\theta}, \quad (4)$$

where ${}^x\alpha_{\text{A/B}}$ are fractionation factors between two reservoirs, A and B:

$${}^xR_{\text{A}} = {}^x\alpha_{\text{A/B}} {}^xR_{\text{B}}. \quad (5)$$

The factors, $^{33}\theta$ and $^{36}\theta$, are called mass-dependent exponents or slopes. For equilibrium exchange reactions, $^{33}\theta$ and $^{36}\theta$ are approximately 0.515 and 1.90, respectively but can deviate from these values at the sub-percent level (Hulston and Thode, 1965b; Farquhar et al., 2003) (see Skaron and Wolfsberg, 1980; Deines, 2003 for a special case at isotopic cross-over temperature). Slightly larger magnitude variations of $^{33}\theta$ and $^{36}\theta$ at the percent level can be produced by different types of kinetically controlled fractionation mechanisms such as diffusion, effusion, or gravitational separation (Craig, 1968; Craig et al., 1988; Young et al., 2002).

We define capital delta values as (Angert et al., 2003; Ono et al., 2003)

$$\Delta^{33}\text{S} = \delta^{33}\text{S}' - {}^{33}\theta_{\text{ref}} \delta^{34}\text{S}' \quad (6)$$

and

$$\Delta^{36}\text{S} = \delta^{36}\text{S}' - {}^{36}\theta_{\text{ref}} \delta^{34}\text{S}'. \quad (7)$$

In this definition, the value $\Delta^{33}\text{S}$ (and $\Delta^{36}\text{S}$) represents deviation of $\delta^{33}\text{S}'$ (and $\delta^{36}\text{S}'$) from a *reference* line defined by ${}^{33}\theta_{\text{ref}}$ (and ${}^{36}\theta_{\text{ref}}$). We use ${}^{33}\theta_{\text{ref}}$ and ${}^{36}\theta_{\text{ref}}$ values of 0.515 and 1.90, respectively, to be representative of a variety of reactions operating with a range of product and reactant species (Hulston and Thode, 1965a,b) although the chosen values do not apply necessarily to isotope fractionation by a specific process (Luz and Barkan, 2005). The definitions used by Farquhar et al. (2000a) (i.e., $\Delta^{33}\text{S} = \delta^{33}\text{S} - 1000 \times [(1 + \delta^{34}\text{S})^{0.515} - 1]$) yield practically identical values ex-

cept for large positive or negative $\delta^{34}\text{S}$ values (Miller, 2002; Ono et al., 2003, appendix).

One of the advantages of above definition of $\Delta^{33}\text{S}$ is that these values can be normalized to the CDT (Cañon Diablo Troilite) scale (or any other scale) by a simple addition without approximation. For instance

$$\Delta^{33}\text{S}_{\text{sample/CDT}} = \Delta^{33}\text{S}_{\text{sample/reference}} + \Delta^{33}\text{S}_{\text{reference/CDT}}, \quad (8)$$

where subscript *reference* refers to laboratory working reference SF_6 , that often has measurable $\Delta^{33}\text{S}$ value with respect to CDT.

2.2. Multiple sulfur isotope systematics in $\delta^{34}\text{S}$ vs. $\Delta^{33}\text{S}$ coordinates

On plots of $\delta^{34}\text{S}$ vs. $\Delta^{33}\text{S}$, the relative placement of the data for two sulfur pools, A and B, related by a fractionation mechanism $A - B$, gives information about $^{33}\theta_{A-B}$ and the magnitude of the fractionation, $^{34}\alpha_{A/B}$. If the measured $^{33}\theta_{A-B}$ is equal to the chosen value of $^{33}\theta_{\text{ref}}$, such as when isotope equilibrium is attained between A and B, the pair of sulfur reservoirs will have the same $\Delta^{33}\text{S}$ value (Fig. 1A). If the $^{33}\theta_{A-B}$ of the fractionation process differs from the value of $^{33}\theta_{\text{ref}}$, such as when the sulfur pool A is produced by diffusion of the pool B, the pair of sulfur reservoirs will have different values of $\Delta^{33}\text{S}$ (Fig. 1B).

It is important to realize that mixing is non-linear in these coordinates (Young et al., 2002; Assonov and Brenninkmeijer, 2005; Luz and Barkan, 2005). During mixing ($A + B \rightarrow C$), because mixing lines are curves in $\delta^{34}\text{S}$ vs. $\Delta^{33}\text{S}$ plots, a new sulfur pool (C) will have a lower $\Delta^{33}\text{S}$ than initial sulfur pools (Fig. 1C). This non-linear effect also applies to a branching process where two or more reservoirs are produced from a single reservoir. This branching process produces new reservoirs where both products are more positive in $\Delta^{33}\text{S}$ than their starting material as long as $^{33}\theta_{A-B} \approx 0.515$. Note that this non-linear effect is not a mathematical artifact. Although mixing is expressed linearly when we define $\Delta^{33}\text{S}$ by traditional delta scales (i.e., $\Delta^{33}\text{S} \equiv \delta^{33}\text{S} - 0.515 \delta^{34}\text{S}$) isotope fractionation becomes non-linear in traditional definition of $\Delta^{33}\text{S}$.

The magnitude of the effect on $\Delta^{33}\text{S}$ during mixing ($A + B \rightarrow C$) is given as

$$\Delta^{33}\text{S}_C - \Delta^{33}\text{S}_B = \left[\ln(^{32}f_A(^{34}\alpha_{A/B}^{^{33}\theta} - 1) + 1) - ^{33}\theta_{\text{ref}} \cdot \ln(^{32}f_A(^{34}\alpha_{A/B} - 1) + 1) \right] \times 1000, \quad (9)$$

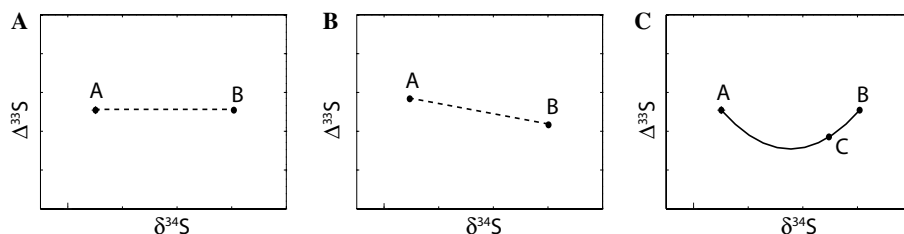


Fig. 1. Triple isotope systematics in $\delta^{34}\text{S}$ vs. $\Delta^{33}\text{S}$ plots. (A) Illustrates a case where A and B are in isotope equilibrium with $^{33}\theta_{A-B} = ^{33}\theta_{\text{ref}}$. (B) When $^{33}\theta_{A-B} < ^{33}\theta_{\text{ref}}$, (C) mixing of reservoirs A and B to form C with $^{33}\theta_{A-B} = ^{33}\theta_{\text{ref}}$.

where $^{32}f_A$ is the ^{32}S normalized mixing ratio of the two initial sulfur reservoirs (i.e., $^{32}f_A = ^{32}\text{S}_A / (^{32}\text{S}_A + ^{32}\text{S}_B)$) (see Appendix A for derivation). As expected, the effect is largest when $f = 0.5$ (i.e., 1:1 mixing). When $f = 0.5$, the effect is -0.120 , -0.082 , -0.052‰ for $^{34}\alpha_A$ of 0.94, 0.95, and 0.96, respectively. As we will see in the later section, such values are measurable by using isotope ratio measurements by a SF_6 method. The effect is relatively large for $\Delta^{36}\text{S}$ ($+0.82$, $+0.56$, and $+0.36\text{‰}$ for $^{34}\alpha_A$ of 0.94, 0.95, and 0.96, respectively), and is a mirror image compared to $\Delta^{33}\text{S}$. Mixing two isotope pools results in sulfur compositions with higher $\Delta^{36}\text{S}$, and branching reactions produce new reservoirs that are more negative in $\Delta^{36}\text{S}$ (when $^{36}\theta_{A-B} \approx 1.9$). These principles apply to natural systems and are the fundamental reason why $\Delta^{33}\text{S}$ and $\Delta^{36}\text{S}$ measurements of natural systems have the potential to provide constraints that are independent of and complementary to those provided by $\delta^{34}\text{S}$ alone.

2.3. Reaction branching and measured θ values for biological processes

Farquhar et al. (2003) reported $^{33}\theta$ value for sulfate reduction (0.5117 ± 0.001) by *Achaeglobus fulgidus*. This value is smaller than the one expected for inorganic chemical equilibrium between sulfate and sulfide at temperature between 0 and 100 °C (0.5148 ± 0.002). For oxygen isotope system, $^{17}\theta$ values during respiration (e.g., by plants and humans) have been studied extensively, and yielded 0.518 ± 0.001 for terratrium experiments (Angert et al., 2003; Luz and Barkan, 2005). This also is significantly smaller than the values defined by rocks of 0.525 ± 0.001 (Miller et al., 1999) and meteoric water of 0.528 ± 0.002 (Meijer and Li, 1998).

Farquhar et al. (2003) applied Rees' (1973) model to multiple-sulfur isotope system and suggested that measured θ value can be explained as a result of biological flow network even when intrinsic enzymatic reactions have θ values identical to thermodynamic equilibrium. This multiple isotope systematics can be treated as a series of branching reactions, and reviewed below. The simplest example for enzymatic reaction can be written as



where substrate (S) binds to enzyme (E) followed by catalysis ($*k_3$) and dissociation (k_5) steps to yield product (P),

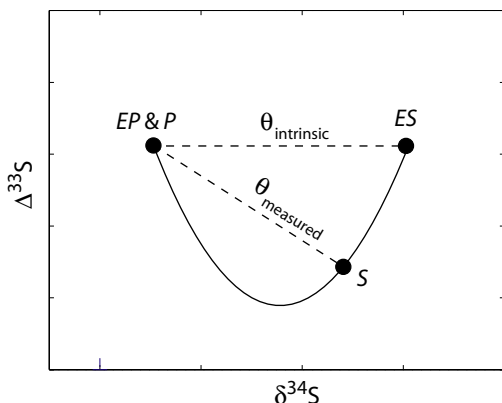


Fig. 2. The isotope branching model for a simple enzymatic reaction discussed in text. Isotopic composition of starting substrate (S) lies on a mixing line (solid line) between intermediate (ES) and product (EP and P). Measured slope between starting substrate and product ($\theta_{\text{measured}} = \theta_{\text{P-S}}$) is different from that intrinsic to the enzymatic reaction ($\theta_{\text{intrinsic}} = \theta_{\text{EP-ES}}$).

and only the catalysis step is assumed to induce isotope effects with fractionation factor, $^x\alpha_3$ (Northrop, 1975). Overall, the fractionation factor that we normally measure ($^x\alpha_{\text{P/S}}$) is different from that intrinsic to the catalysis ($^x\alpha_3$); the intrinsic fractionation factor is only expressed when isotope sensitive step is rate limiting (Rees, 1973; Northrop, 1975). Farquhar et al. (2003) showed that it is also true that the slope for the overall reaction ($\theta_{\text{S-P}}$) can be different from that intrinsic to the catalysis ($\theta_{\text{ES-EP}}$).

This isotope systematics can be explained by a branching reaction scheme discussed above, and shown graphically in Fig. 2. At steady state, the isotope mass-balance is maintained at the branching point around ES such that the flow of material into ES (along k_1 with isotope composition of S) is balanced by the flow out of ES (along k_2 and k_3 , with isotope compositions of ES and EP, respectively). In this branching reaction, the measured slope ($\theta_{\text{P-S}}$) is not identical to the one intrinsic to the catalysis ($\theta_{\text{EP-ES}}$), and this is one of the fundamental reasons why θ values expressed for biological processes are different from that expected for equilibrium processes. Actual biological processes are not as simple as this example by having more than one branching and isotope sensitive steps, as dealt by Farquhar et al. (2003) for sulfate reduction network. As one may see, deviations of θ values from equilibrium θ values are not exclusive to biological processes but characteristic to any processes that involves reaction intermediates.

3. High precision analysis for four sulfur isotopes

3.1. Analytical techniques

A laser fluorination SF_6 system was developed to measure sulfur isotope ratios ($^{33}\text{S}/^{32}\text{S}$, and $^{34}\text{S}/^{32}\text{S}$) at the Geophysical Laboratory (GL), and detailed descriptions of the fluorination techniques can be found in earlier papers

(Rumble et al., 1993; Hu et al., 2003). Modifications of the gas chromatographic purification line and installation of a new, quadruple collector, isotope ratio mass spectrometer (Thermo-Electron MAT 253) have enabled high precision measurements of ^{33}S and ^{36}S in this study, and are described in detail here.

Sulfur hexafluoride is produced by the reaction of pyrite or silver sulfide with elemental fluorine at 25–30 torr within a laser fluorination manifold at GL. A CO_2 laser is used to heat silver sulfide and an excimer laser (KrF: 248 nm) is used to photo-ablate spots on mineral grain surfaces for in situ analysis (Hu et al., 2003). Sulfur hexafluoride contains unwanted contaminants that are formed during laser fluorination. Some contaminants interfere with the ion beams of SF_5^+ and some potentially may damage the mass spectrometer (e.g., HF and C–H–F compounds). Thus, purification of SF_6 by gas chromatography (GC) is a critical step for high precision analysis. Due to the low abundance of ^{36}S (0.02%), and mass-interference on mass 131 ($^{36}\text{SF}_5^+$), analysis of ^{36}S had been challenging (Hulston and Thode, 1965b; Hoering, 1989; Gao and Thiemens, 1991). In order to facilitate GC separation, a dual GC system was developed, which consists of two GC columns and three multiport valves that are electronically controlled for semiautomatic operation (Fig. 3). The fluorination product is injected first onto a series of packed column (molecular sieve 5 Å, 60–80 mesh, 1/8 in. OD, and 2.0 m, linked with Hayesep Q, 1/8 in. OD, 80–100 mesh, and 2.4 m) at a He flow rate of 25 mL/min and at 100 °C. The SF_6 elutes at ca. 4 min from the first column. The GC effluent is monitored by a thermal conductivity detector (TCD) and a time window that contains SF_6 is injected onto the second column by switching a multiport valve. The stationary phase of the second column is a Hayesep Q (1/8 in. OD, 80–100 mesh, and 2.0 m) operated with a He flow rate at 25 mL/min. The SF_6 is, again, detected by a TCD and trapped by liquid nitrogen at -196 °C in the collection loop (Fig. 3). The first column is continuously back-flushed between analyses to avoid co-elution of contaminants onto subsequent samples.

Analyses of silver sulfide at the stable isotope laboratory of the University of Maryland College Park (UMCP) were conducted by loading silver sulfide (wrapped in aluminum foil) into externally heated nickel metal vessels of internal volume of ~ 10 cm³. The vessels were then filled with 75–150 torr of F_2 , and heated to ~ 300 °C overnight. The GC purification system uses one 1/8 in. OD, 4.8 m Hayesep Q column operated at 50 °C. The column is back-flushed at 150 °C for 15 min after each GC run to avoid elution of contaminants onto subsequent samples. The product SF_6 is purified by passing the SF_6 through the column two times.

Both laboratories use Thermo-Electron MAT 253 isotope ratio mass-spectrometers. The instruments are equipped with faraday cups that allow simultaneous determination of masses 127, 128, 129, and 131 ($^{32}\text{SF}_5^+$, $^{33}\text{SF}_5^+$, $^{34}\text{SF}_5^+$, and $^{36}\text{SF}_5^+$, respectively).

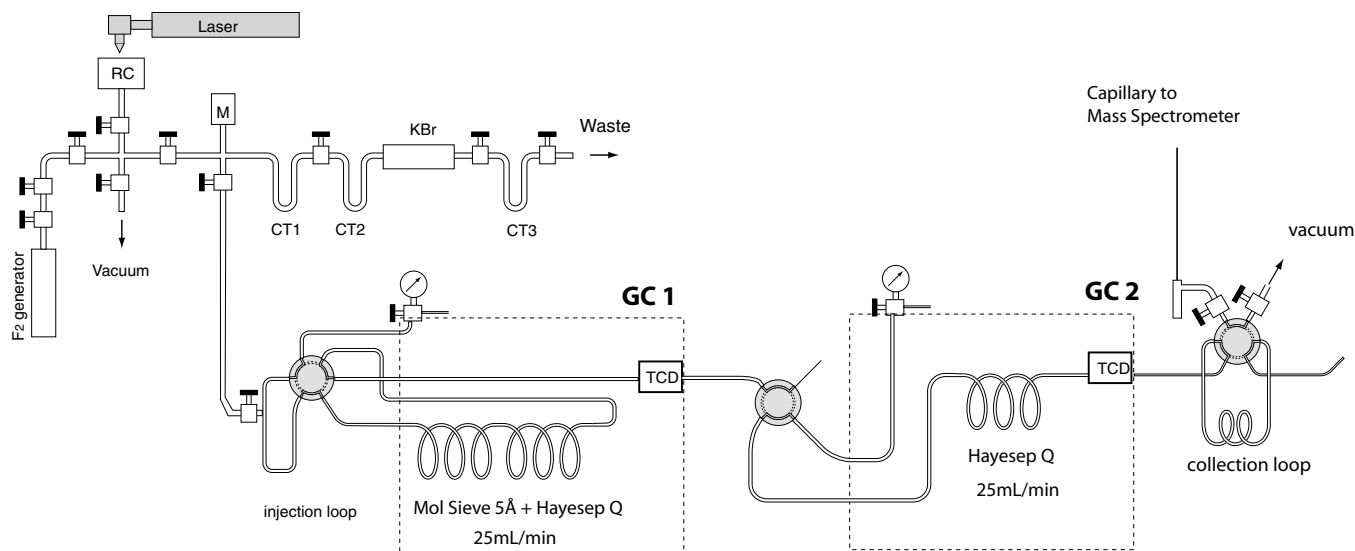


Fig. 3. Outline of the Geophysical Laboratory laser fluorination dual-GC manifold for high precision multiple-sulfur isotope analysis. RC, reaction chamber; CT, cold traps; M, capacitance manometer; TCD, thermal conductivity detector.

3.2. Precision and accuracy

A troilite inclusion from the Cañon Diablo meteorite (CDT) was measured in situ by an excimer laser (KrF) at GL. Seven measurements of CDT yield standard deviation (1σ) of 0.30, 0.013, 0.17‰ for $\delta^{34}\text{S}$, $\Delta^{33}\text{S}$ and $\Delta^{36}\text{S}$, respectively (Table 1). Three IAEA reference Ag_2S (S-1, S-2, and S-3) were measured at both GL and UMCP for inter-laboratory comparison of accuracy and precision. Tables 1 and 2 list the $\delta^{\text{X}}\text{S}$ values with respect to house reference gases at GL and UMCP. The data in Tables 1 and 2 represent complete analyses, including fluorination, gas-purification, and mass-spectrometry measurements. Typical precisions for $\delta^{33}\text{S}$, $\delta^{34}\text{S}$, and $\delta^{36}\text{S}$ are a few tenths of permil. Because most errors in isotope ratio measurements are mass-dependent, the internal (intra-laboratory) precision for $\Delta^{33}\text{S}$ and $\Delta^{36}\text{S}$ are better than that for $\delta^{\text{X}}\text{S}$, typically 0.01 and 0.2‰ (1σ), respectively (Fig. 4A, Tables 1 and 2). Least squares regression of the $\delta^{33}\text{S}'$ and $\delta^{34}\text{S}'$ data for individual samples in Tables 1 and 2 (CDT, S-1, S-2, and S-3) yields slopes that are not exactly 0.515. These calculated slopes, however, are not statistically different from 0.515 when the mass spectrometric measurement uncertainties (1σ of ~ 0.014 and ~ 0.008 for $\delta^{33}\text{S}'$ and $\delta^{34}\text{S}'$, respectively) are taken into account for each data point.

Cañon Diablo Troilite (CDT) was historically used as a reference material for sulfur isotopic analyses (Jensen and Nakai, 1962; Hulston and Thode, 1965b) until a new reference material IAEA S-1 (Ag_2S) was introduced. The supply of CDT was increasingly limited and, moreover it is isotopically heterogeneous (Beaudoin et al., 1994). A new reference scale, Vienna-CDT (V-CDT) is defined by the reference material, IAEA S-1, having $\delta^{34}\text{S}_{\text{V-CDT}}$ of -0.3‰ (Robinson, 1993). Because $\delta^{33}\text{S}$ and $\delta^{36}\text{S}$ (and thus, $\Delta^{33}\text{S}$ and $\Delta^{36}\text{S}$) have not been defined for V-CDT, we normalize $\delta^{34}\text{S}$, $\Delta^{33}\text{S}$ and $\Delta^{36}\text{S}$ values with respect to IAEA S-1

Table 1

The multiple-sulfur isotope ratios of CDT and IAEA reference materials measured at the Geophysical Laboratory

Sample	$\delta^{33}\text{S}$	$\delta^{34}\text{S}$	$\delta^{36}\text{S}$	$\Delta^{33}\text{S}$	$\Delta^{36}\text{S}$
CDT	2.317	4.613	8.78	-0.056	0.00
CDT	2.530	5.050	9.37	-0.067	-0.24
CDT	2.538	5.012	9.57	-0.040	0.03
CDT	2.738	5.380	10.23	-0.029	-0.02
CDT	2.581	5.111	9.32	-0.048	-0.41
CDT	2.603	5.129	9.54	-0.036	-0.22
CDT	2.885	5.665	10.90	-0.028	0.10
Average	2.60	5.14	9.67	-0.043	-0.11
1σ	0.16	0.30	0.64	0.013	0.17
IAEA S-1	2.650	5.027	8.52	0.064	-1.04
IAEA S-1	2.300	4.355	7.19	0.060	-1.09
IAEA S-1	2.623	4.967	8.51	0.068	-0.94
Average	2.52	4.78	8.07	0.064	-1.02
1σ	0.19	0.37	0.76	0.004	0.08
IAEA S-2	14.058	27.444	52.27	0.017	-0.49
IAEA S-2	13.785	26.916	51.34	0.012	-0.39
IAEA S-2	13.821	26.988	51.41	0.012	-0.47
Average	13.89	27.12	51.67	0.014	-0.45
1σ	0.15	0.29	0.52	0.003	0.05
IAEA S-3	-14.183	-27.451	-52.84	0.051	-1.40
IAEA S-3	-14.222	-27.514	-53.07	0.044	-1.52
IAEA S-3	-14.335	-27.734	-53.30	0.046	-1.33
IAEA S-3	-13.764	-26.653	-51.66	0.053	-1.71
IAEA S-3	-14.394	-27.843	-53.22	0.044	-1.04
Average	-14.18	-27.44	-52.81	0.048	-1.40
1σ	0.25	0.47	0.67	0.004	0.25

The isotope ratios are reported with respect to the laboratory working reference SF_6 at GL.

and list them in Table 3 for inter-laboratory comparison. The data in Table 3 show that $\Delta^{33}\text{S}$ values obtained at GL and UMCP are consistent within intra-laboratory pre-

Table 2
The multiple-sulfur isotope ratios of IAEA reference materials measured at the University of Maryland College Park

Sample	$\delta^{33}\text{S}$	$\delta^{34}\text{S}$	$\delta^{36}\text{S}$	$\Delta^{33}\text{S}$	$\Delta^{36}\text{S}$
IAEA S-1	-2.452	-4.921	-10.05	0.086	-0.73
IAEA S-1	-2.562	-5.135	-10.52	0.086	-0.79
IAEA S-1	-2.627	-5.261	-10.75	0.086	-0.78
IAEA S-1	-2.570	-5.135	-10.43	0.078	-0.70
IAEA S-1	-2.437	-4.929	-10.00	0.105	-0.66
IAEA S-1	-2.461	-4.970	-9.68	0.102	-0.26
IAEA S-1	-2.532	-5.057	-10.26	0.075	-0.68
IAEA S-1	-2.554	-5.124	-10.30	0.088	-0.60
IAEA S-1	-2.462	-4.946	-9.99	0.088	-0.62
IAEA S-1	-2.574	-5.166	-10.43	0.090	-0.64
IAEA S-1	-2.583	-5.158	-10.55	0.076	-0.78
IAEA S-1	-2.600	-5.184	-10.80	0.073	-0.98
IAEA S-1	-2.577	-5.166	-10.61	0.088	-0.83
IAEA S-1	-2.564	-5.125	-10.52	0.079	-0.81
IAEA S-1	-2.455	-4.942	-9.75	0.093	-0.39
Average	-2.53	-5.08	-10.31	0.086	-0.68
1 σ	0.06	0.11	0.33	0.009	0.17
IAEA S-2	8.810	17.122	32.73	0.029	-0.05
IAEA S-2	8.936	17.369	33.28	0.028	0.02
IAEA S-2	8.873	17.250	33.02	0.026	-0.01
IAEA S-2	9.078	17.657	33.98	0.023	0.16
IAEA S-2	9.109	17.680	33.97	0.041	0.10
IAEA S-2	8.951	17.389	33.33	0.032	0.03
IAEA S-2	9.005	17.499	33.39	0.030	-0.12
IAEA S-2	9.155	17.776	34.07	0.039	0.02
IAEA S-2	9.041	17.566	33.67	0.032	0.03
IAEA S-2	8.979	17.419	33.40	0.045	0.05
IAEA S-2	8.943	17.373	33.85	0.033	0.56
IAEA S-2	8.928	17.349	33.52	0.030	0.29
IAEA S-2	8.946	17.397	33.08	0.023	-0.22
IAEA S-2	8.941	17.363	33.17	0.036	-0.07
Average	8.98	17.44	33.46	0.032	0.06
1 σ	0.09	0.18	0.40	0.006	0.19
IAEA S-3	-19.212	-37.068	-70.32	0.054	-1.15
IAEA S-3	-19.235	-37.130	-70.54	0.063	-1.26
IAEA S-3	-19.274	-37.215	-70.75	0.069	-1.32
IAEA S-3	-19.221	-37.083	-70.44	0.053	-1.25
IAEA S-3	-19.171	-37.014	-70.26	0.067	-1.19
IAEA S-3	-19.244	-37.181	-70.49	0.082	-1.11
IAEA S-3	-19.276	-37.196	-70.25	0.057	-0.81
IAEA S-3	-19.273	-37.189	-70.19	0.057	-0.77
IAEA S-3	-19.329	-37.302	-70.30	0.060	-0.66
IAEA S-3	-19.204	-37.099	-69.75	0.078	-0.47
IAEA S-3	-19.156	-37.021	-69.65	0.086	-0.52
IAEA S-3	-19.262	-37.168	-70.76	0.056	-1.42
IAEA S-3	-19.266	-37.206	-70.21	0.072	-0.76
IAEA S-3	-19.253	-37.163	-70.79	0.063	-1.46
IAEA S-3	-19.264	-37.194	-70.64	0.068	-1.24
IAEA S-3	-19.197	-37.074	-69.75	0.072	-0.52
Average	-19.24	-37.14	-70.32	0.066	-0.99
1 σ	0.04	0.08	0.36	0.010	0.34

The isotope ratios are reported with respect to the laboratory working reference SF₆ at UMCP.

cisions (i.e., $\pm 0.01\%$); IAEA S-2 and S-3 have $\Delta^{33}\text{S}_{\text{S-1}}$ values of $-0.05 \pm 0.01\%$ and $-0.02 \pm 0.01\%$, respectively. Note that data for IAEA reference materials were obtained within a month period at GL whereas UMCP data

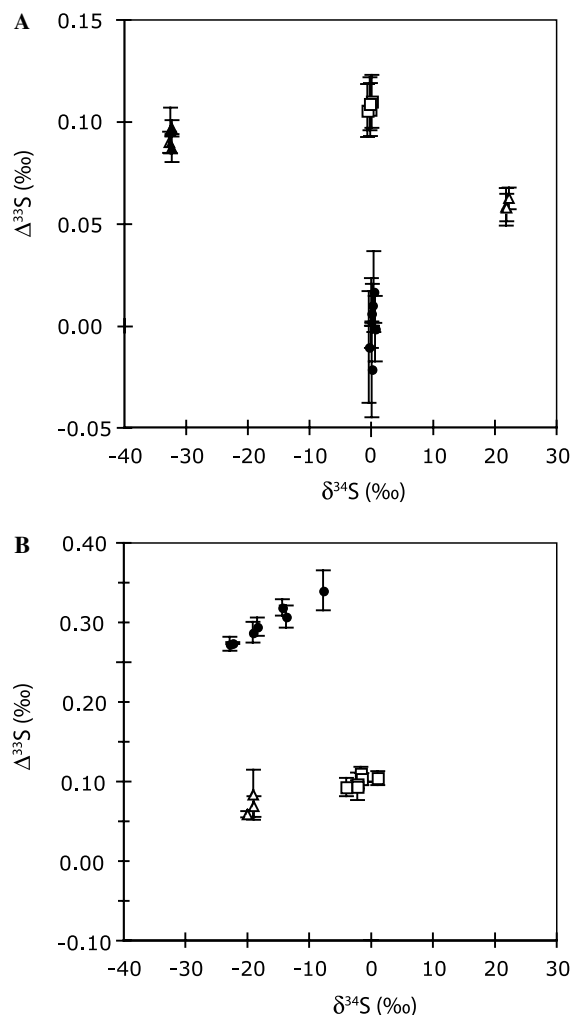


Fig. 4. Plot of $\delta^{34}\text{S}$ vs. $\Delta^{33}\text{S}$ for sulfate and sulfide analyzed in this study. (A) CDT and IAEA reference materials, ●: CDT; □: IAEA S-1; △: IAEA S-2; and ▲: IAEA S-3, (B) pyritized fossils and pyritic-graphitic schist. ●: Jurassic Ammonite; □: Devonian Brachiopods; and △: Silurian Schist. Error bars represent standard deviation (1 σ) of mass-spectrometer runs (typically consist of four measurement cycles).

represent measurements of over a year in order to illustrate long-term reproducibility. These values are also consistent with values reported in Table 8 of Ding et al. (2001) obtained at Institute for Reference Materials and Measurements at Geel, Belgium (calculated by using $\Delta^{33}\text{S}$ definition in this paper). The value of $\Delta^{33}\text{S}$ obtained by previous study at GL (Hu et al., 2003) is also consistent for S-2 (-0.04% with respect to S-1) but not for S-3 (0.03%). The data in Table 3 also show that CDT has $\Delta^{33}\text{S}_{\text{S-1}}$ value of $-0.10 \pm 0.01\%$, which is reported by three laboratories (GL, UCSD, and Geel). Hu et al. (2003) also reported similar but slightly lower values for CDT of -0.13% with respect to IAEA S-1.

The values of $\Delta^{36}\text{S}_{\text{S-1}}$ for IAEA S-2 are 0.57 and 0.74%, and those of S-3 are -0.38 and -0.31 for GL and UMCP, respectively. These values agree well within our current intra-laboratory reproducibility of ca. $\pm 0.2\%$. If we take $\Delta^{36}\text{S}_{\text{CDT}}$ of S-1 to be -0.91% , all three IAEA reference

Table 3

The multiple-sulfur isotopic compositions ($\delta^{34}\text{S}$, $\Delta^{33}\text{S}$, and $\Delta^{36}\text{S}$) for three IAEA reference materials (S-1, S-2, and S-3) measured at the Geophysical Laboratory (GL) and University of Maryland College Park (UMCP)

	GL-CIW	UMCP	Hu et al. ^a	Ding et al. ^b	Gao and Thiemens ^c
$\delta^{34}\text{S}_{\text{S-1}}$ (‰)					
CDT	0.35 (7)		0.46 (11)		0.27 (14)
S-1	0.00 (3)	0.00 (15)	0.00 (13)	0.00	0.00 (11)
S-2	22.23 (3)	22.64 (14)	22.84 (12)	22.95	
S-3	-32.07 (5)	-32.22 (16)	-31.84 (10)	-32.37	
$\Delta^{33}\text{S}_{\text{S-1}}$ (‰)					
CDT	-0.107		-0.13	-0.10	-0.10
S-1	0.000	0.000	0.00	0.00	0.00
S-2	-0.050	-0.054	-0.04	-0.05	
S-3	-0.016	-0.020	0.03	-0.02	
$\Delta^{36}\text{S}_{\text{S-1}}$ (‰)					
CDT	0.91				0.49
S-1	0.00	0.00			0.00
S-2	0.57	0.74			
S-3	-0.38	-0.31			

All isotope ratios are normalized with respect to IAEA S-1. Also listed are values calculated from published data from Hu et al. (2003), Ding et al. (2001), and Gao and Thiemens (1993a).

^a From Table 3 of Hu et al. (2003) with unpublished data for two decimal units for $\delta^{34}\text{S}$.

^b From Table 8 of Ding et al. (2001) data obtained at IRMM, Geel.

^c Table 1 of Gao and Thiemens (1993a). The values for $\Delta^{33}\text{S}$ and $\Delta^{36}\text{S}$ are recalculated according to definition used in this paper.

materials have negative values of $\Delta^{36}\text{S}_{\text{CDT}}$, which is expected because of their positive values of $\Delta^{33}\text{S}$ with respect to CDT.

4. Analyses of Phanerozoic sedimentary pyrite

Multiple sulfur isotopic compositions of pyritized fossils and pyrite in carbonaceous schist were measured by in situ fluorination with an excimer laser (248 nm), in order to document the natural range of $\Delta^{33}\text{S}$ and $\Delta^{36}\text{S}$ for biogenic pyrite of Phanerozoic age. Laser pits approximately 400 μm in diameter and 300 μm deep produced $\sim 4 \mu\text{mol}$ of SF_6 .

4.1. Materials

4.1.1. Pyritized ammonite, *Cosmoceras* sp., Jurassic

This is a specimen of pyritized ammonite, *Cosmoceras* sp. from the Volga River region, Russia. The age of the ammonite is Collovian (163–169 Ma), Jurassic. The specimen (ca. 35 mm in size) was cut into half and the associated carbonate mineral was dissolved with dilute hydrochloric acid.

4.1.2. Pyritized brachiopods from the silica formation, Devonian

The specimen of pyritized brachiopods (*Eospirifer* sp.) from the Devonian Silica formation (Stewart, 1927) is taken from a quarry of the Medusa Cement Company, Silica, Sylvania Township, OH. The shells of brachiopods are pyritized and a specimen (ca. 3 cm) was cut in half and polished for analysis.

4.1.3. Metamorphic schist, Silurian

The sample is a chlorite grade graphite-sulfide-rich schist from the Silurian Waterville Formation exposed in south-central Maine, USA (Rumble et al., 1991; Oliver et al., 1992). The sample contains euhedral pyrite grains of up to 5 mm size. Polished sections were prepared for isotope analysis.

4.2. Results

The single specimen of pyritized ammonite yields variation in $\delta^{34}\text{S}$ ranging from -23.0 to -6.1 ‰ (Fig. 5), and $\Delta^{33}\text{S}$ ranges from 0.27 to 0.34‰ (Table 4). The $\Delta^{33}\text{S}$ values are among the largest measured for non-atmospheric Phanerozoic materials (Fig. 4B). The $\Delta^{36}\text{S}$ is also the most negative for Phanerozoic sulfide, ranging from -1.9 to -2.4 ‰. The values of $\Delta^{33}\text{S}$ correlate with $\delta^{34}\text{S}$. These data are characterized by a slope of 0.5194 ± 0.0003 (1σ) instead of 0.515. Other sedimentary pyrites are also characterized by positive $\Delta^{33}\text{S}$ and negative $\Delta^{36}\text{S}$ values with respect to CDT. Six analyses of pyritized brachiopods yield $\delta^{34}\text{S}$, $\Delta^{33}\text{S}$, and $\Delta^{36}\text{S}$ of -4.1 to 0.9, 0.09 to 0.11, and -0.5 to -0.6 ‰, respectively. Three analyses of pyrites in Silurian schist yield $\delta^{34}\text{S}$, $\Delta^{33}\text{S}$ and $\Delta^{36}\text{S}$ values of -19.1 to -20.1 , 0.06 to 0.08, and -0.4 to -0.6 ‰, respectively (Table 4; Fig. 4B).

A plot of $\Delta^{33}\text{S}$ vs. $\Delta^{36}\text{S}$ measured for Phanerozoic sedimentary sulfur-bearing materials reveals an apparent linear correlation with a slope of ca. -6.9 (Fig. 6). The correlation is particularly striking because of the negative correlation between $\Delta^{33}\text{S}$ and $\Delta^{36}\text{S}$ in Archean sulfide and sulfate minerals reported by Farquhar et al. (2000a). There is a discrepancy between the Phanerozoic and Archean correlations, however, in that the Archean analyses record a slope of -0.9 on a plot of $\Delta^{33}\text{S}$ vs. $\Delta^{36}\text{S}$ (Fig. 7). Deducing the origin of the large difference in slope between the Phanerozoic and Archean data is important and will be discussed below.

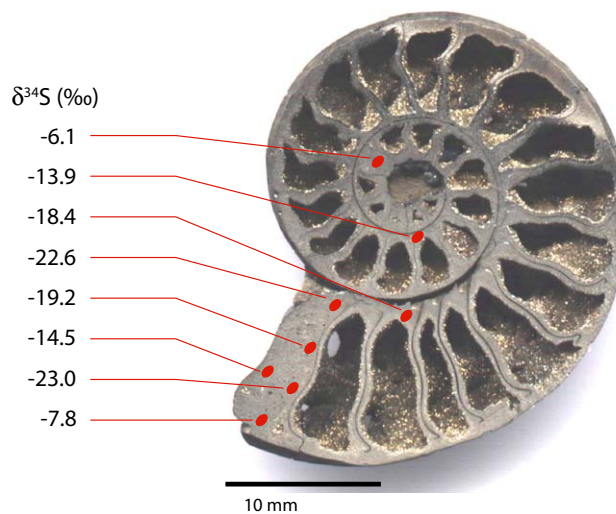


Fig. 5. Pyritized Jurassic ammonite, *Cosmoceras* sp. and its $\delta^{34}\text{S}$ determined by in situ fluorination analysis.

Table 4
High precision multiple-sulfur isotope measurements of sedimentary sulfide of Phanerozoic age

$\delta^{33}\text{S}$	$\delta^{34}\text{S}$	$\delta^{36}\text{S}$	$\Delta^{33}\text{S}$	$\Delta^{36}\text{S}$
<i>Cosmoceras sp. Jurassic</i>				
-3.705	-7.833	-17.19	0.338	-2.40
-7.178	-14.496	-29.64	0.316	-2.35
-11.636	-22.983	-45.26	0.271	-2.14
-9.665	-19.225	-38.40	0.285	-2.28
-11.411	-22.551	-44.40	0.270	-2.08
-6.878	-13.896	-28.28	0.305	-2.10
-9.259	-18.446	-36.61	0.286	-1.92
-2.834	-6.143	-13.65	0.336	-2.04
<i>Brachiopods, Silica formation, Devonian</i>				
0.569	0.907	1.08	0.102	-0.64
-0.803	-1.769	-3.96	0.109	-0.60
-0.742	-1.636	-3.71	0.101	-0.61
-0.442	-1.047	-2.56	0.098	-0.57
-2.040	-4.133	-8.36	0.090	-0.52
-1.097	-2.307	-4.84	0.091	-0.46
<i>Silurian Schist 83-41-AA3-55</i>				
-9.842	-19.177	-36.47	0.081	-0.36
-9.808	-19.083	-36.41	0.066	-0.48
-10.324	-20.057	-38.30	0.056	-0.55

All isotope ratios are normalized to CDT.

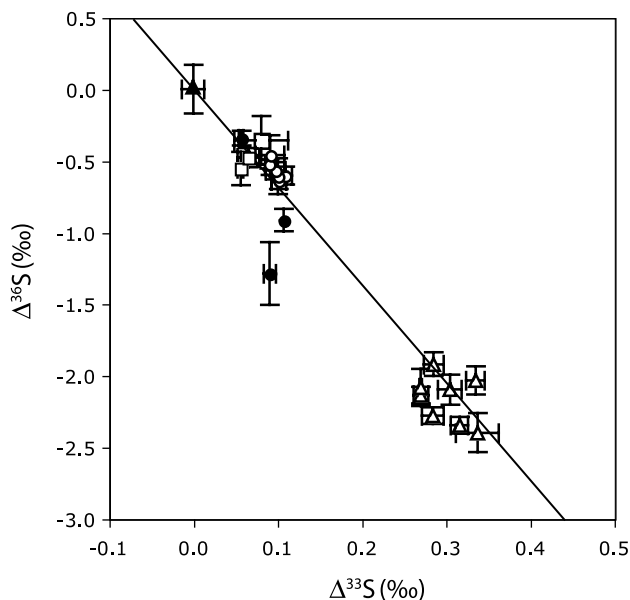


Fig. 6. A plot of $\Delta^{33}\text{S}$ vs. $\Delta^{36}\text{S}$ reported in this study. ▲: CDT; △: Jurassic Ammonite; ○: Devonian Brachiopods; □: Silurian Schist; and ●: IAEA reference materials. The line represents $\Delta^{36}\text{S}/\Delta^{33}\text{S}$ of -6.85 .

5. Discussion

5.1. $\Delta^{33}\text{S}$ of primordial sulfur

Most meteorite materials (e.g., enstatite and ordinary chondrite, troilite inclusion in iron meteorite, ureilites, and moon rocks) show small variation of $\delta^{34}\text{S}$ as well as $\Delta^{33}\text{S}$ and $\Delta^{36}\text{S}$ (Jensen and Nakai, 1962; Hulston and

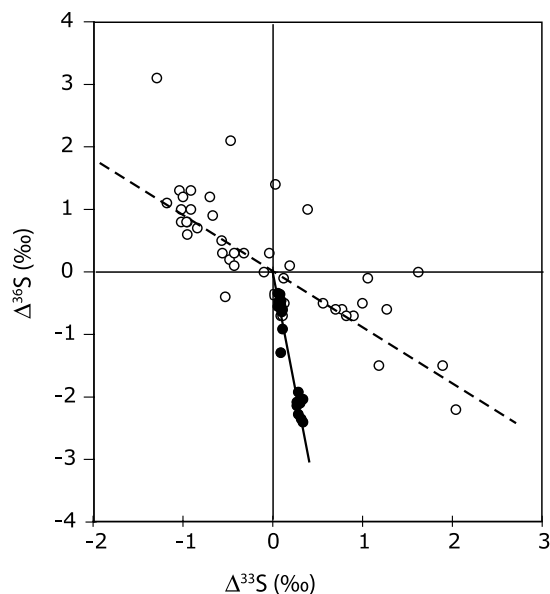


Fig. 7. Plot of $\Delta^{33}\text{S}$ and $\Delta^{36}\text{S}$ for Phanerozoic samples measured in this study (●), compared to mass-independent sulfur isotope signatures for rocks older than 2450 Ma reported in Farquhar et al. (2000a) (○). The dashed and solid lines are $\Delta^{36}\text{S}/\Delta^{33}\text{S}$ of -0.9 and -6.85 , respectively.

Thode, 1965b; Thode and Rees, 1971; Rees and Thode, 1974; Gao and Thiemens, 1991; Gao and Thiemens, 1993a,b; Farquhar et al., 2000b). The reported values of $\Delta^{33}\text{S}_{\text{CDT}}$ and $\Delta^{36}\text{S}_{\text{CDT}}$ for these materials typically are ± 0.05 and ± 0.1 ‰, respectively. Much larger $\Delta^{33}\text{S}$ and $\Delta^{36}\text{S}$ values are reported from some components of trace sulfur in metal phases of iron meteorites (Hulston and Thode, 1965a; Gao and Thiemens, 1991), sulfonic acid in carbonaceous chondrites (Cooper et al., 1997), and sulfide and sulfate sulfur in Martian meteorites (Farquhar et al., 2000c; Greenwood et al., 2000). Excess ^{33}S and ^{36}S in metal phases of iron meteorites is thought to be an effect of nuclear spallation (Gao and Thiemens, 1991), and mass-independent isotope signatures in Martian meteorites and sulfonic acid in carbonaceous chondrite are thought to be a result of gas phase photochemical reactions (Cooper et al., 1997; Farquhar et al., 2000c). Because the materials with non-zero $\Delta^{33}\text{S}$ and $\Delta^{36}\text{S}$ values in meteorites represent a minor component of planetary sulfur, a starting assumption has been to assume that the $\Delta^{33}\text{S}$ (and $\Delta^{36}\text{S}$) of bulk Earth would be close to the grand average of the bulk meteorite composition (i.e., close to CDT; Farquhar et al., 2002). This is also supported by near CDT value of $\Delta^{33}\text{S}$ (0.03 ± 0.04 ‰) reported for sulfur in peridotite xenoliths (Farquhar et al., 2002).

The three IAEA Ag_2S reference materials examined here (S-1, S-2, and S-3) are terrestrial in origin. IAEA S-1 and S-3 originate from Mississippi valley type Zn–Pb deposits in Triassic dolomite located in the Silesian-Cracovian area, South Poland, and are prepared from sphalerite (ZnS) (S. Halas pers. comm.). IAEA S-2 is prepared from gypsum that is precipitated from present day seawater in evaporite ponds in New Zealand (Robinson, 1993). All three IAEA

reference materials and the Phanerozoic biogenic pyrite, yield positive $\Delta^{33}\text{S}$ and negative $\Delta^{36}\text{S}$ with respect to CDT. Our starting hypothesis is that all of these terrestrial materials originate from sulfur pools that were produced as a result of processes that partitioned sulfur along branching pathways, and can be traced back to the primordial sulfur (with $\delta^{33}\text{S} = \delta^{34}\text{S} = \delta^{36}\text{S} = 0\text{‰}$). In the following sections, we will describe the causes of these effects in more detail.

5.2. Multiple sulfur isotope systematics in a closed system

Sedimentary pyrite is produced by bacterial reduction of seawater sulfate, and often is characterized by a wide range of $\delta^{34}\text{S}$ values. The range of variation can be due to a variety of reasons, including recycling of sulfur within microbial communities (Canfield and Teske, 1996) and irreversible reactions in a closed system (that lead to Rayleigh distillation effects) (Ohmoto and Goldhaber, 1997). Sediments below bioturbation zones are used as typical examples of partly closed systems when the sulfate reduction rate is faster than the supply of sulfate by diffusion (Ohmoto, 1992; Ohmoto and Goldhaber, 1997).

We interpret the large positive $\Delta^{33}\text{S}$ and negative $\Delta^{36}\text{S}$ values and highly variable $\delta^{34}\text{S}$ (-23 to -6‰) for the pyritized ammonite to reflect bacterial sulfate reduction in a closed system. The isotope systematics in a closed system process, reactant (A) \rightarrow product (B), can be described by the Rayleigh distillation equation, where evolution of the isotope ratio of the reactant (xR_A) can be derived as

$$\ln\left(\frac{{}^xR_A}{{}^xR_{A,i}}\right) = ({}^x\alpha - 1) \ln({}^{32}f_A), \quad (11)$$

where ${}^xR_{A,i}$ is the initial isotopic ratios of the reactant (${}^x\text{S}/{}^{32}\text{S}$), and ${}^{32}f_A$ is the fraction of ${}^{32}\text{S}$ remaining (Mariotti et al., 1981). Using modified delta notation, Eq. (11), can be written as

$$\delta^x S'_A = ({}^x\alpha - 1) \ln({}^{32}f_A) \times 1000 + \delta^x S'_{A,i} \quad (12)$$

where $\delta^x S'_{A,i}$ is the isotopic composition of the initial reactant. The $\Delta^{33}\text{S}$ of the reactant (A) can be derived as a function of ${}^{34}\alpha$, ${}^{33}\theta$ and ${}^{32}f_A$

$$\Delta^{33}S_A = \{({}^{34}\alpha^{33}\theta - 1) - {}^{33}\theta_{\text{ref}} \cdot ({}^{34}\alpha - 1)\} \cdot \ln({}^{32}f_A) \times 1000 + \Delta^{33}S_{A,i} \quad (13)$$

and isotopic composition of the reactant will evolve following the relationship:

$${}^{33}\gamma = \frac{\delta^{33}S'_A - \delta^{33}S'_{A,i}}{\delta^{34}S'_A - \delta^{34}S'_{A,i}} = \frac{({}^{33}\alpha - 1) \cdot \ln({}^{32}f_A)}{({}^{34}\alpha - 1) \cdot \ln({}^{32}f_A)} = \frac{{}^{34}\alpha^{33}\theta - 1}{{}^{34}\alpha - 1}. \quad (14)$$

Note that in a distillation process, the observed slope in $\delta^{33}\text{S}'$ vs. $\delta^{34}\text{S}'$ coordinates (${}^{33}\gamma$) is different from that intrinsic to the reaction (${}^{33}\theta$) (Blunier et al., 2002; Angert et al., 2004; Kaiser et al., 2004). Eq. (14) shows that ${}^{33}\gamma$ is independent of ${}^{32}f_A$ and is only a function of ${}^{34}\alpha$ and ${}^{33}\theta$.

The ${}^{33}\gamma$ value approaches ${}^{33}\theta$ when ${}^{34}\alpha$ approaches to unity. Rayleigh distillation can be viewed as a series of branching reaction where the starting pool branches to product and remaining reactant in each step. Rayleigh processes, thus, will effectively amplify the non-linearity effect by repeating branching reactions.

If the sulfur isotopic composition of starting material (i.e., Jurassic seawater sulfate or local sulfate in the basin) is known, we can constrain both ${}^{34}\alpha$ and ${}^{33}\theta$ by measurements of $\delta^{34}\text{S}$ and $\Delta^{33}\text{S}$. We use a $\delta^{34}\text{S}$ value of seawater of $+16\text{‰}$ (Holser and Kaplan, 1966; Claypool et al., 1980), and assume $\Delta^{33}\text{S}$ of $+0.057$ (from $\Delta^{33}\text{S}$ of IAEA S-2, discussed in the next section). The best fit was obtained for ${}^{34}\alpha$ and ${}^{33}\theta$ of 0.947 and 0.512, respectively, for the given isotopic composition of starting sulfate (Fig. 8). The value of ${}^{33}\theta$ of 0.512 is similar to the one extracted for sulfate reduction by *A. fulgidus* reported in Farquhar et al. (2003). The fractionation factor (${}^{34}\alpha$) of 0.947 is within the range of fractionation factors between sulfate and sulfide observed in nature (e.g., Canfield and Teske, 1996) although the maximum fractionation factor by sulfate reducing bacteria in culture experiments is 46‰ (or ${}^{34}\alpha \approx 0.954\text{‰}$) (Kaplan and Rittenberg, 1964). The largest uncertainty in the discussion is in the values assigned for $\Delta^{33}\text{S}$ and $\delta^{34}\text{S}$ of local seawater in the basin, which can be constrained if sulfate sulfur (e.g., gypsum or carbonate associated sulfate) is available. The discussion illustrates how non-zero values of $\Delta^{33}\text{S}$ for sedimentary pyrite can be produced by mass-dependent processes involving distillation. It can be seen that $\Delta^{33}\text{S}$ is sensitive to closed system processes even when $\delta^{34}\text{S}$ approaches that of starting material. The model demonstrates the potential of the multiple-sulfur isotope system for providing additional insights into microbial sulfate reduction in natural systems.

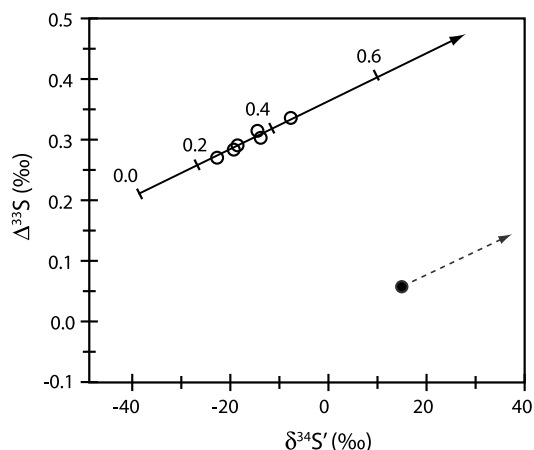


Fig. 8. Model calculation for sulfate reduction in a closed system in $\delta^{34}\text{S}'$ vs. $\Delta^{33}\text{S}$ with data for pyritized Ammonite (O). The evolution of remaining seawater sulfate (dashed line) and product sulfide (solid line) is calculated for ${}^{34}\alpha = 0.947$ and ${}^{33}\theta = 0.512$, with starting sulfate (●: SS) of $\delta^{34}\text{S} = +16\text{‰}$, $\Delta^{33}\text{S} = +0.057$, which is shown in solid circle. The number on the line is a fraction of sulfate converted to sulfide.

5.3. Multiple sulfur isotope systematics in an open system: $\Delta^{33}\text{S}$ of seawater sulfate

The $\delta^{34}\text{S}$ record of the seawater sulfate has long been used to constrain the ocean sulfur budget (Holser and Kaplan, 1966; Garrels and Lerman, 1981; Holser et al., 1989; Strauss, 1997). These models use isotope mass-balance for the seawater sulfate reservoir, which can be written in terms of the modified delta notation

$$\delta^{34}\text{S}'_{\text{SS}} = -\ln(^{32}f_{\text{PY}}(^{34}\alpha_{\text{PY/SS}} - 1) + 1) \times 1000 + \delta^{34}\text{S}'_{\text{IN}}, \quad (15)$$

where subscripts SS and IN refer to $\delta^{34}\text{S}'$ of seawater sulfate and integrated sulfate flux into the sulfate reservoir (mostly riverine sulfate), $^{32}f_{\text{PY}}$ is a fraction of sedimentary sulfide burial over total sulfur flux in and out of the oceanic sulfate reservoir, and $^{34}\alpha_{\text{PY/SS}}$ is isotope fractionation factor (for $^{34}\text{S}/^{32}\text{S}$) during sedimentary sulfide formation (see Appendix B for derivation). The $\Delta^{33}\text{S}$ of seawater sulfate is

$$\Delta^{33}\text{S}_{\text{SS}} = \left[-\ln(^{32}f_{\text{PY}}(^{34}\alpha_{\text{PY/SS}}^{^{33}\theta_{\text{PY-SS}}} - 1) + 1) + ^{33}\theta_{\text{ref}} \cdot \ln(^{32}f_{\text{PY}}(^{34}\alpha_{\text{PY/SS}} - 1) + 1) \right] \times 1000 + \Delta^{33}\text{S}_{\text{IN}}, \quad (16)$$

where $^{33}\theta_{\text{PY-SS}}$ is the mass-dependent exponent for isotope fractionation during sedimentary pyrite formation.

The Eqs. (15) and (16) can be solved for $^{34}\alpha_{\text{PY/SS}}$ and $^{32}f_{\text{PY}}$ for given values of $\delta^{34}\text{S}'$, $\Delta^{33}\text{S}$ and $^{33}\theta_{\text{PY-SS}}$ (Figs. 9 and 10, and Table 5). Following the Garrels and Lerman model, we assume $\delta^{34}\text{S}'_{\text{IN}} = 7.65\text{‰}$, and use $\delta^{34}\text{S}_{\text{SS}} = 19\text{‰}$. The $\Delta^{33}\text{S}_{\text{SS}}$ is $+0.057 \pm 0.015\text{‰}$, which is $\Delta^{33}\text{S}$ of IAEA S-2, with respect to CDT, measured at GL. We further assume $\Delta^{33}\text{S}_{\text{IN}}$ to be $+0.012\text{‰}$. This is calculated as a simple mixture of the seawater sulfate reservoir and bulk Earth (i.e., CDT) to have $\delta^{34}\text{S}$

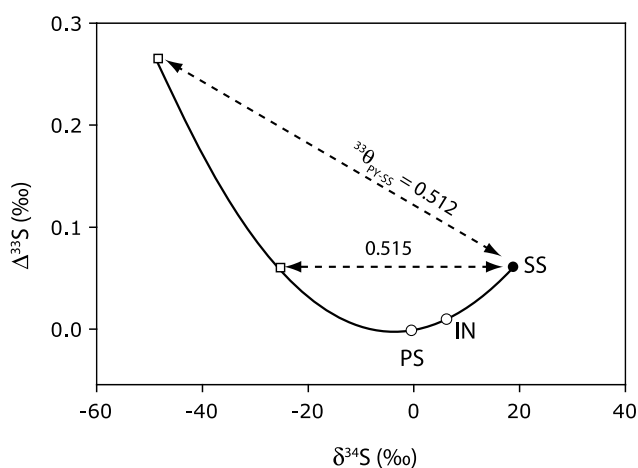


Fig. 9. Graphical representation of the global branching model for the oceanic sulfate budget. Primordial sulfur (PS) reservoir branches to make seawater sulfate (SS) and sedimentary sulfide reservoirs (\square). Mean isotopic composition of sedimentary sulfide can be derived as a function of $^{33}\theta_{\text{PY-SS}}$. The $\Delta^{33}\text{S}$ of sulfur flux into the ocean (IN) is assumed to be a mixture of primordial sulfur and seawater sulfate (i.e., plots on a mixing line). Triple-sulfur isotope system can be used to close the global sulfur budget.

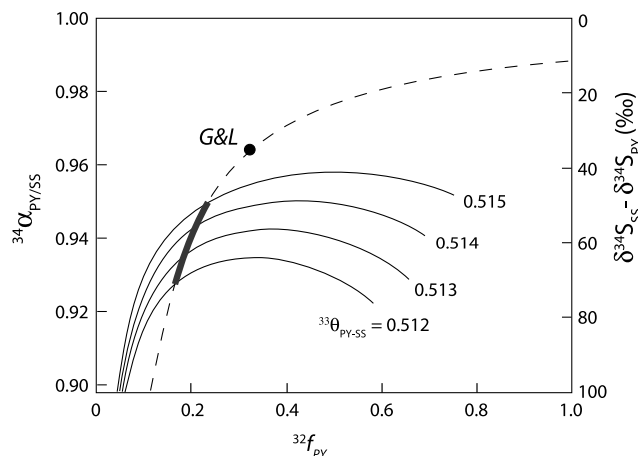


Fig. 10. The model of oceanic sulfate budget from $\delta^{34}\text{S}$ and $\Delta^{33}\text{S}$ of seawater sulfate. Dashed line represents a combination of $\delta^{34}\text{S}_{\text{SS}} - \delta^{34}\text{S}_{\text{PY}}$ and $^{32}f_{\text{PY}}$ that produce seawater sulfate with $\delta^{34}\text{S}$ of 19.0‰ (e.g., Garrels and Lerman, 1981), solid lines are combinations of $\delta^{34}\text{S}_{\text{SS}} - \delta^{34}\text{S}_{\text{PY}}$ and $^{32}f_{\text{PY}}$ that yield measured $\Delta^{33}\text{S}$ seawater sulfate of $+0.057\text{‰}$ (four lines are for different $^{33}\theta_{\text{PY-SS}}$ values). The values used by Garrels and Lerman (1981) is shown as *G&L*. Bold solid line represents a condition that satisfies both $\delta^{34}\text{S}$ and $\Delta^{33}\text{S}$ constraints.

Table 5

Model result for global seawater sulfate budget

$^{33}\theta_{\text{PY-SS}}$	0.515	0.514	0.513	0.512
$^{34}\alpha_{\text{PY/SS}}$	0.958	0.950	0.943	0.935
$^{32}f_{\text{PY}}$	0.26	0.22	0.19	0.17
$\delta^{34}\text{S}_{\text{SS}} - \delta^{34}\text{S}_{\text{PY}} (\text{‰})$	43	51	58	66
$\Delta^{33}\text{S}_{\text{PY}} (\text{‰})$	0.057	0.108	0.175	0.258

Predicted isotopic fractionation factor ($^{34}\alpha_{\text{PY-SS}}$) and fractional sulfide burial ($^{32}f_{\text{PY}}$), $\delta^{34}\text{S}_{\text{SS}} - \delta^{34}\text{S}_{\text{PY}}$, and model $\Delta^{33}\text{S}$ value of sulfide as a function of $^{33}\theta_{\text{PY-SS}}$.

of $+7.65\text{‰}$. One of the major unknown is the value of $^{33}\theta_{\text{PY-SS}}$, which represents a *global average* value between sedimentary sulfide and seawater sulfate. As demonstrated by high $\Delta^{33}\text{S}$ values for a pyritized ammonite, the value of $^{33}\theta_{\text{PY-SS}}$ may differ locally as a function of the nature of the depositional environments (e.g., closed or open with respect to sulfate) and biosynthetic pathways of sedimentary sulfide formation (e.g., relative contribution of sulfur disproportionation; Johnston et al., 2005). We used the range of values from 0.515 to 0.512 for the canonical value of mass-dependent exponents and values obtained for microbial sulfate reduction (Farquhar et al., 2003), respectively.

Fig. 9 shows a graphical representation of our global branching model of the global sulfur budget. A fundamental assumption is that mixing of surface sulfur reservoirs (sedimentary sulfate and sulfide) would yield the isotope composition of primordial sulfur (i.e., $\delta^{34}\text{S} = \Delta^{33}\text{S} = 0$). Seawater sulfate and average sedimentary sulfide would plot on a mixing line that is represented as a solid curved line. Our new estimate suggests the $\delta^{34}\text{S}$ difference ($\delta^{34}\text{S}_{\text{SS}} - \delta^{34}\text{S}_{\text{PY}} \approx (1 - ^{34}\alpha_{\text{PY-SS}}) \times 1000$) between sulfide and sulfate to be $43\text{--}66\text{‰}$ for $^{33}\theta_{\text{PY-SS}}$ values from 0.515–0.512 (Fig. 10 and Table 5). This value is larger than

the 35‰ used by Garrels and Lerman (1981) for their $\delta^{34}\text{S}$ mass balance model. The larger value is consistent with a recent compilation of $\delta^{34}\text{S}$ differences between sulfate and sulfide in modern sediments (average 38.5‰) and much of the Mesozoic (32.5–54.2‰) (Strauss, 1997). The corresponding fraction of sulfide burial (f_{PY}) is between 0.24 and 0.16 (Fig. 10 and Table 5), smaller than the earlier estimate of 0.33 (Garrels and Lerman, 1981).

A potential application of multiple isotope study is to incorporate $\Delta^{33}\text{S}$ into the model of the Phanerozoic sulfur cycle. It is a tradition since Garrels and Lerman (1981) that the isotope mass-balance model of the Phanerozoic sulfur cycle model (Berner et al., 1983; Berner and Canfield, 1989; Berner, 2001) uses a fixed value of $^{34}\alpha_{\text{PY/SS}}$ for the entire Phanerozoic. Recent models, however, implemented $^{34}\alpha_{\text{PY/SS}}$ as a variable related to atmospheric oxygen levels although the relationship between oxygen levels and $^{34}\alpha_{\text{PY/SS}}$ is not well established (Berner, 2001; Berner, 2005). Thus, application of $\Delta^{33}\text{S}$ systematics for a non-steady state model may put additional constraints on the Phanerozoic sulfur cycle, which may be ultimately related to the history of the atmospheric oxygen in the Phanerozoic era (e.g., Berner, 2001).

5.4. $\Delta^{36}\text{S}$ and $\Delta^{33}\text{S}$ systematics

We have focused our discussion on triple sulfur isotope systematics (^{32}S – ^{33}S – ^{34}S). Additional information may be obtained, however, by including ^{36}S in the analysis. The $\Delta^{36}\text{S}/\Delta^{33}\text{S}$ ratios of Phanerozoic sulfide are -6.1 to -8.1 , -5.0 to -6.3 and -4.4 to -9.8 for Jurassic Ammonite, Devonian Brachiopods, and Silurian schist, respectively, and those for IAEA reference materials are -8.5 , -6.2 , and -14 , for S-1, S-2, and S-3, respectively. These ratios depend highly on the reference zero-point (i.e., measured isotope ratio of CDT). An apparent negative correlation in $\Delta^{33}\text{S}$ vs. $\Delta^{36}\text{S}$ suggests processes governing $\Delta^{36}\text{S}$ variations are similar to those of $\Delta^{33}\text{S}$ (Fig. 6). It is not likely that the correlation is due to analytical artifacts from mass-interferences on either ^{32}S or ^{34}S (i.e., $^{32}\text{SF}_5^+$, and $^{34}\text{SF}_5^+$). Although these two mass-interferences are expected to produce correlated errors in both $\Delta^{33}\text{S}$ and $\Delta^{36}\text{S}$, random addition of ^{32}S and ^{34}S would produce errors that are characterized by $\Delta^{36}\text{S}/\Delta^{33}\text{S}$ ratios of -1.9 and $+3.7$, respectively (Appendix C).

For a simple mixing process, the ratio $\Delta^{36}\text{S}/\Delta^{33}\text{S}$ can be written as (from Eq. (9)):

$$\frac{\Delta^{36}\text{S}_{\text{C}} - \Delta^{36}\text{S}_{\text{B}}}{\Delta^{33}\text{S}_{\text{C}} - \Delta^{33}\text{S}_{\text{B}}} = \frac{\ln(^{32}f_{\text{A}}(^{34}\alpha_{\text{A/B}}^{36}\theta - 1) + 1) - ^{36}\theta_{\text{ref}} \cdot \ln(^{32}f_{\text{A}}(^{34}\alpha_{\text{A/B}} - 1) + 1)}{\ln(^{32}f_{\text{A}}(^{34}\alpha_{\text{A/B}}^{33}\theta - 1) + 1) - ^{33}\theta_{\text{ref}} \cdot \ln(^{32}f_{\text{A}}(^{34}\alpha_{\text{A/B}} - 1) + 1)}. \quad (17)$$

When $^{34}\alpha_{\text{A/B}} \approx 1$ and $^x\theta \approx ^x\theta_{\text{ref}}$, Eq. (17) can be approximated as (see Appendix A for derivation)

$$\frac{\Delta^{36}\text{S}_{\text{C}} - \Delta^{36}\text{S}_{\text{B}}}{\Delta^{33}\text{S}_{\text{C}} - \Delta^{33}\text{S}_{\text{B}}} \approx \frac{-(1/2)^{36}\theta(^{36}\theta - 1)^{32}f_{\text{A}}(^{32}f_{\text{A}} - 1)(^{34}\alpha_{\text{A/B}} - 1)^2}{-(1/2)^{33}\theta(^{33}\theta - 1)^{32}f_{\text{A}}(^{32}f_{\text{A}} - 1)(^{34}\alpha_{\text{A/B}} - 1)^2} = \frac{^{36}\theta(^{36}\theta - 1)}{^{33}\theta(^{33}\theta - 1)}. \quad (18)$$

The mixing ratio ($^{32}f_{\text{B}}$) and fractionation factor ($^{34}\alpha - 1$) cancels for the ratio $\Delta^{36}\text{S}/\Delta^{33}\text{S}$, and this yields -6.85 when values of 0.515 and 1.90 are used for $^{33}\theta$ and $^{36}\theta$, respectively. This is consistent with the data presented in this paper (Fig. 6). Eqs. (16) and (17) show that the exact $\Delta^{36}\text{S}/\Delta^{33}\text{S}$ ratio depends upon values of $^{33}\theta$ and $^{36}\theta$ (and $^{33}\theta_{\text{ref}}$ and $^{36}\theta_{\text{ref}}$) as well as $^{34}\alpha$ and $^{32}f_{\text{A}}$. Natural systems may be composed of a number of branching and mixing processes, and thus, are expected to show variable $\Delta^{36}\text{S}/\Delta^{33}\text{S}$ ratios. Other solutions may exist for $\Delta^{36}\text{S}/\Delta^{33}\text{S}$ systematics in nature and further modeling and measurements may be necessary to determine the full range of variations in the ratio $\Delta^{36}\text{S}/\Delta^{33}\text{S}$ for mass-dependent process.

5.5. Implications to Archean sulfur isotope record

Sulfide and sulfate minerals in Archean sedimentary rocks are known to have a wide range of $\Delta^{33}\text{S}$ of $+8.2$ to -2.5 ‰ (Farquhar et al., 2000a; Mojzsis et al., 2003; Ono et al., 2003). The large variation in $\Delta^{33}\text{S}$ is difficult to explain by mass-dependent effects as discussed in this paper. It requires unreasonably large isotope fractionation (α significantly differ from 1) and/or special distillation mechanism to amplify the effect. Therefore, large non-zero $\Delta^{33}\text{S}$ values in Archeans rocks are most consistent with mass-independent isotope effect (i.e., $^{33}\theta$ significantly different from 0.515) that was acquired during photochemical reactions in the atmosphere (Farquhar et al., 2000a; Pavlov and Kasting, 2002; Ono et al., 2003). Furthermore, the $\Delta^{36}\text{S}/\Delta^{33}\text{S}$ ratio seen in Phanerozoic sulfide is different from that seen in the Archean rock record (Fig. 7; Farquhar et al., 2000a), indicating a fundamental difference in the origins of $\Delta^{33}\text{S}$ and $\Delta^{36}\text{S}$ between Phanerozoic and Archean sulfur.

It is of critical importance to recover a detailed sulfur isotope record between 2.45 and 2.0 Ga. The sulfur isotope system records the change in the sulfur cycle in response to the rise of oxygen in this critical period of the Earth's history (Farquhar et al., 2000a; Wing et al., 2002; Bekker et al., 2004). This time period is called Stage II by Farquhar et al. (2003), and is characterized by much smaller magnitudes of $\Delta^{33}\text{S}$ and $\Delta^{36}\text{S}$ compared to values in rocks older than 2.5 Ga. Reported values of $\Delta^{33}\text{S}$ and $\Delta^{36}\text{S}$ for the Stage II (Farquhar et al., 2000a; Bekker et al., 2004) are generally within the range of values presented in this paper for Phanerozoic sulfur. Quadruple sulfur isotope system is advantageous compared to triple oxygen isotope system because the ratio $\Delta^{36}\text{S}/\Delta^{33}\text{S}$ may be used to distinguish mass-independent and mass-dependent contributions. Therefore, it is of fundamental impor-

tance to characterize $\Delta^{36}\text{S}/\Delta^{33}\text{S}$ systematics for mass-dependent and the Archean mass-independent processes as well as to make careful and precise measurement of both $\Delta^{33}\text{S}$ and $\Delta^{36}\text{S}$ of sulfur in the rocks of age 2.45 and 2.0 Ga, in order to elucidate the origin of small magnitude $\Delta^{33}\text{S}$ of this critical time of the Earth's history.

6. Conclusion

We report $\Delta^{33}\text{S}$ and $\Delta^{36}\text{S}$ values of international reference materials and sedimentary sulfide of Phanerozoic age. We propose that the observed relationship among $\delta^{34}\text{S}$, $\Delta^{33}\text{S}$, and $\Delta^{36}\text{S}$ can be explained by mass-dependent isotope effect where small $\Delta^{33}\text{S}$ (and $\Delta^{36}\text{S}$) are produced as a result of functional difference between the power law dependence of mass-dependent isotope fractionation and isotopic mass balance. We discuss how these small $\Delta^{33}\text{S}$ and $\Delta^{36}\text{S}$ variations can be used to gain additional information for tracing biogeochemical sulfur cycles. New constraints can be gained for the global sulfur cycle, in particular, regarding the magnitude of fractionation between seawater sulfate and sedimentary sulfide, and the depositional environment of sedimentary sulfide formation. The non-zero $\Delta^{33}\text{S}$ and $\Delta^{36}\text{S}$ values produced by mass-dependent processes may yield characteristic $\Delta^{36}\text{S}/\Delta^{33}\text{S}$ ratios that may be used as a tool to decouple signatures of mass-independent and mass-dependent isotope fractionation isotope effects for small magnitude $\Delta^{33}\text{S}$. Therefore, high precision quadruple sulfur isotope analysis holds a great potential to gain new insights into sulfur biogeochemical cycles in the present day and geologic past.

Acknowledgments

The authors thank Marilyn Fogel, George Cody, Albert Colman, and Pat Shanks for valuable comments on earlier manuscripts, and Roger Husted and Patti Dixon (Thermo Finnigan) for assistance on mass-spectrometer, Christian Henning, James Scott, and Robert Hazen for supplying materials and valuable discussions, and John Jamieson (UMCP) for sharing mass-spectrometer time. Reviews by H. Bao, B. Luz, and an anonymous reviewer and D. Canfield are greatly appreciated. S. Ono acknowledges support from Agouron Institute. The financial supports of the National Science Foundation (EAR 0125096 and EAR 021593 to Rumble, EAR-0034382 and EAR 0003419 to Farquhar), NASA Cosmochemistry (NAG 512948 to Rumble and NAG 512350 to Farquhar), the Jet Propulsion Laboratory (contract 1213932 to P.G. Conrad, M.L. Fogel, W.T. Huntress, K. Nealson, and D. Rumble), NASA Astrobiology Institute, and the Carnegie Institution of Washington are also acknowledged with gratitude.

Associate editor: Donald E. Canfield

Appendix A. Multiple sulfur isotope systematics in mixing and branching processes

Consider mixing of two sulfur reservoirs to make one new reservoir (i.e., $A + B \rightarrow C$). For isotope mass-balance

$${}^x m_A + {}^x m_B = {}^x m_C, \quad (\text{a1.1})$$

where m is the amount (e.g., number of moles) of sulfur in each reservoir (A, B, and C) and x refers to isotopes ($x = 32, 33, 34, 36$). Because ${}^{34}R = {}^{34}m/{}^{32}m$ and ${}^{34}m_A + {}^{34}m_B = {}^{34}m_C$

$${}^{34}R_A {}^{32}m_A + {}^{34}R_B {}^{32}m_B = {}^{34}R_C {}^{32}m_C \quad (\text{a1.2})$$

and

$${}^{34}\alpha_{A/B} {}^{32}f_A {}^{34}R_B + (1 - {}^{32}f_A) {}^{34}R_B = {}^{34}R_C, \quad (\text{a1.3})$$

where ${}^{32}f_A = {}^{32}m_A/{}^{32}m_C$, and ${}^{34}\alpha_{A/B} = {}^{34}R_A/{}^{34}R_B$. Rearranging (a1.3):

$${}^{34}R_C = ({}^{32}f_A ({}^{34}\alpha_{A/B} - 1) + 1) {}^{34}R_B. \quad (\text{a1.4})$$

Dividing both side by ${}^{34}R_{\text{reference}}$, and taking logarithm

$$\delta^{34}\text{S}'_C = \ln({}^{32}f_A ({}^{34}\alpha_{A/B} - 1) + 1) \times 1000 + \delta^{34}\text{S}'_B. \quad (\text{a1.5})$$

For ${}^{33}\text{S}$

$$\delta^{33}\text{S}'_C = \ln({}^{32}f_A ({}^{33}\alpha_{A/B} - 1) + 1) \times 1000 + \delta^{33}\text{S}'_B. \quad (\text{a1.6})$$

When ${}^{33}\alpha = {}^{34}\alpha^{33\theta}$ (i.e., $\Delta^{33}\text{S}_A = \Delta^{33}\text{S}_B$)

$$\Delta^{33}\text{S}_C - \Delta^{33}\text{S}_B = \left[\ln({}^{32}f_A ({}^{34}\alpha_{A/B}^{33\theta} - 1) + 1) - {}^{33}\theta \cdot \ln({}^{32}f_A ({}^{34}\alpha_{A/B} - 1) + 1) \right] \times 1000. \quad (\text{a1.7})$$

We used ${}^{32}\text{S}$ -normalized mixing ratio (${}^{32}f_A$) because it simplifies the formulation without approximation.

Because

$$\ln(x + 1) = x - \frac{x^2}{2} + \frac{x^3}{3} - \frac{x^4}{4} \dots \quad (\text{a1.8})$$

and

$$\alpha^\theta - 1 = \theta(\alpha - 1) + \frac{1}{2}\theta(\theta - 1)(\alpha - 1)^2 + \frac{1}{6}\theta(\theta - 1)(\theta - 2)(\alpha - 1)^3 + \dots \quad (\text{a1.9})$$

We can approximate Eq. (a1.7) by dropping the term higher than $(\alpha - 1)^2$

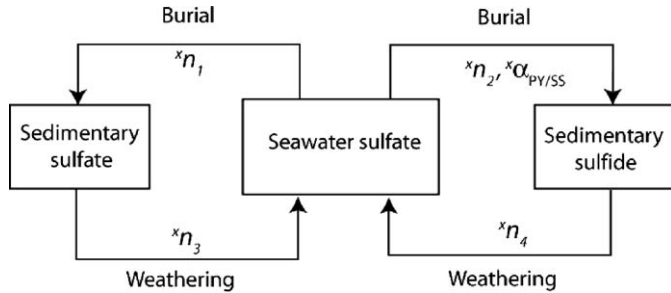
$$\begin{aligned} & \ln(f(\alpha^\theta - 1) + 1) - \theta \cdot \ln(f(\alpha - 1) + 1) \\ & \approx f(\alpha^\theta - 1) - \frac{1}{2}f^2(\alpha^\theta - 1)^2 - \theta f(\alpha - 1) + \frac{1}{2}\theta f^2(\alpha - 1)^2 \\ & \approx \theta f(\alpha - 1) + \frac{1}{2}\theta f(\theta - 1)(\alpha - 1)^2 \\ & \quad - \frac{1}{2}f^2\theta^2(\alpha - 1)^2 - \theta f(\alpha - 1) + \frac{1}{2}\theta f^2(\alpha - 1)^2 \\ & = -\frac{1}{2}\theta(\theta - 1)f(f - 1)(\alpha - 1)^2. \end{aligned} \quad (\text{a1.10})$$

Thus, when ${}^{33}\theta = {}^{33}\theta_{\text{ref}}$

$$\Delta^{33}\text{S}_C - \Delta^{33}\text{S}_B \approx -\frac{1}{2}{}^{33}\theta({}^{33}\theta - 1){}^{32}f_A ({}^{32}f_A - 1) \times ({}^{34}\alpha_{A/B} - 1)^2 \times 1000. \quad (\text{a1.11})$$

Appendix B. Multiple sulfur isotope systematics for seawater sulfate cycle

We employed a box model for the Holocene sulfur cycle of Garrels and Lerman (1981) and Holser et al. (1989):



where n_1 , n_2 , n_3 , and n_4 are isotope specific sulfur fluxes into and out of the seawater sulfate reservoir ($x = 32, 33, 34$ or 36). The fluxes n_1 and n_2 represent deposition of sedimentary sulfate (gypsum) and sedimentary sulfide (mostly biogenic pyrite). Major isotope fractionation is associated with deposition of sedimentary sulfide (i.e., bacterial reduction of seawater sulfate) with fractionation factor of $\alpha_{PY/SS}$, and mass-dependent exponent of $^{33}\lambda_{PY-SS}$. Weathering of sulfide and sulfate exposed on land brings sulfur back to the ocean in the form of riverine sulfate fluxes (fluxes n_3 and n_4).

The isotope ratios $^{34}\text{S}/^{32}\text{S}$ for the fluxes n_1 , n_2 , n_3 and n_4 are

$$\frac{^{34}n_1}{^{32}n_1} = ^{34}R_{SS}, \quad \frac{^{34}n_2}{^{32}n_2} = ^{34}\alpha_{PY/SS} ^{34}R_{SS}, \quad \text{and} \quad \frac{^{34}n_3 + ^{34}n_4}{^{32}n_3 + ^{32}n_4} = ^{34}R_{IN}, \quad (\text{a2.1})$$

where $^{34}R_{SS}$ and $^{34}R_{IN}$ are $^{34}\text{S}/^{32}\text{S}$ of seawater sulfate and average weathered sulfur, respectively. The continuity equation for ^{34}S in the seawater reservoir is

$$\begin{aligned} \frac{d^{34}\text{S}_{SS}}{dt} &= -^{34}n_1 - ^{34}n_2 + ^{34}n_3 + ^{34}n_4 \\ &= -^{32}n_1 ^{34}R_{SS} - ^{32}n_2 ^{34}\alpha_{PY/SS} ^{34}R_{SS} + (^{32}n_3 + ^{32}n_4) ^{34}R_{IN}. \end{aligned} \quad (\text{a2.2})$$

At steady state, $d^{34}\text{S}_{SS}/dt = 0$, then

$$^{34}R_{SS} = \frac{^{34}R_{IN}}{^{32}f_{PY}(^{34}\alpha - 1) + 1}, \quad (\text{a2.3})$$

where $^{32}f_{PY}$ is the fraction of ^{32}S deposited as sedimentary sulfide (i.e., $^{32}f_{PY} = ^{32}n_2 / (^{32}n_3 + ^{32}n_4)$). From (a2.3)

$$\delta^{34}\text{S}'_{SS} = -\ln(^{32}f_{PY}(^{34}\alpha_{PY/SS} - 1) + 1) \times 1000 + \delta^{34}\text{S}'_{IN}. \quad (\text{a2.4})$$

Similarly

$$\delta^{33}\text{S}'_{SS} = -\ln(^{32}f_{PY}(^{33}\alpha_{PY/SS} - 1) + 1) \times 1000 + \delta^{33}\text{S}'_{IN}. \quad (\text{a2.5})$$

Because $^{33}\alpha = ^{34}\alpha^{^{33}\theta_{PY-SS}}$, $\Delta^{33}\text{S}$ of the seawater reservoir is

$$\begin{aligned} \Delta^{33}\text{S}_{SS} &= \left[-\ln(^{32}f_{PY}(^{34}\alpha_{PY/SS} ^{^{33}\theta_{PY-SS}} - 1) + 1) \right. \\ &\quad \left. + ^{33}\theta \cdot \ln(^{32}f_{PY}(^{34}\alpha_{PY/SS} - 1) + 1) \right] \times 1000 + \Delta^{33}\text{S}_{IN}. \end{aligned} \quad (\text{a2.6})$$

Appendix C. Artificial $\Delta^{36}\text{S}/\Delta^{33}\text{S}$ from mass-interferences

For mass-spectrometer analysis, the measured isotope ratios (xR_m) are the ratios of minor ions (m/z 128, 129 and 131 for $^{33}\text{SF}_5^+$, $^{34}\text{SF}_5^+$ and $^{36}\text{SF}_5^+$, respectively) to major ion (m/z 127 of $^{32}\text{SF}_5^+$). Thus

$$^xR_m = \frac{x+^{95}I}{^{127}I + ^{127}i}, \quad (\text{a3.1})$$

where x is 33, 34, or 36, $x+^{95}I$ represent true signals from $^x\text{SF}_5^+$ and ^{127}i is a false signal from mass-interference. This translates to $\delta^x\text{S}'$ as

$$\delta^x\text{S}'_m = \delta^x\text{S}'_t + \ln\left(\frac{^{127}I}{^{127}I + ^{127}i}\right) \times 1000, \quad (\text{a3.2})$$

where $\delta^x\text{S}'_m$ and $\delta^x\text{S}'_t$ are measured and true (without interference) values. This will propagate to capital delta value as

$$\begin{aligned} \Delta^{33}\text{S}_m &= \delta^{33}\text{S}'_t + ^{32}\phi - ^{33}\theta_{\text{ref}}(\delta^{34}\text{S}'_t + ^{32}\phi) \\ &= \Delta^{33}\text{S}_t + ^{32}\phi(1 - ^{33}\theta_{\text{ref}}), \end{aligned} \quad (\text{a3.3})$$

where

$$^{32}\phi = \ln\left(\frac{^{127}I}{^{127}I + ^{127}i}\right) \times 1000 \quad (\text{a3.4})$$

and $\Delta^{33}\text{S}_m$ and $\Delta^{33}\text{S}_t$ are measured and true $\Delta^{33}\text{S}$, respectively.

Similar relationship exists for measured and true values for $\Delta^{36}\text{S}$ and this yield following relationship:

$$\frac{\Delta^{36}\text{S}_m - \Delta^{36}\text{S}_t}{\Delta^{33}\text{S}_m - \Delta^{33}\text{S}_t} = \frac{(1 - ^{36}\theta_{\text{ref}}) \cdot ^{32}\phi}{(1 - ^{33}\theta_{\text{ref}}) \cdot ^{32}\phi} \approx -1.86. \quad (\text{a3.5})$$

Because error due to ^{127}I mass-interference cancels out, it is expected to produce characteristic $\Delta^{36}\text{S}/\Delta^{33}\text{S}$ ratio of -1.9 .

Similarly, if there is mass-interferences on ion current 129 (for $^{34}\text{SF}_5^+$), the measured $\delta^{34}\text{S}'_m$ is

$$\delta^{34}\text{S}'_m = \delta^{34}\text{S}'_t + \ln\left(\frac{^{129}I + ^{129}i}{^{129}I}\right) \times 1000. \quad (\text{a3.6})$$

This propagates to the error on $\Delta^{33}\text{S}$ as

$$\begin{aligned} \Delta^{33}\text{S}_m &= \delta^{33}\text{S}'_t - ^{33}\theta_{\text{ref}}(\delta^{34}\text{S}'_t - ^{34}\phi) \\ &= \Delta^{33}\text{S}_t + ^{33}\theta_{\text{ref}} \cdot ^{34}\phi. \end{aligned} \quad (\text{a3.7})$$

Therefore

$$\frac{\Delta^{36}\text{S}_m - \Delta^{36}\text{S}}{\Delta^{33}\text{S}_m - \Delta^{33}\text{S}} = \frac{^{36}\theta_{\text{ref}} \cdot ^{34}\phi}{^{33}\theta_{\text{ref}} \cdot ^{34}\phi} \approx 3.69. \quad (\text{a3.8})$$

Again, mass-interference on 129 ($^{34}\text{SF}_5^+$) cancels for the calculation of the ratio $\Delta^{36}\text{S}/\Delta^{33}\text{S}$.

References

- Angert, A., Cappa, C.D., DePaolo, D.J., 2004. Kinetic O-17 effects in the hydrologic cycle: indirect evidence and implications. *Geochim. Cosmochim. Acta* **68**, 3487–3495.
- Angert, A., Rachmilevitch, S., Barkan, E., Luz, B., 2003. Effects of photorespiration, the cytochrome pathway, and the alternative pathway on the triple isotopic composition of atmospheric O₂ – art. no. 1030. *Global Biogeochem. Cycles* **17**. doi:10.1029/2002GB00.
- Assonov, S.S., Brenninkmeijer, C.A., 2005. Reporting small $\Delta^{17}\text{O}$ values: existing definitions and concepts. *Rapid Commun. Mass Spectrom.* **19**, 627–636.
- Beaudoin, G., Taylor, B.E., Rumble III, D., Thiemens, M., 1994. Variations in the sulfur isotope composition of troilite from the Canon Diablo iron meteorite. *Geochim. Cosmochim. Acta* **58**, 4253–4255.
- Bekker, A., Holland, H.D., Wang, P.L., Rumble, D., Stein, H.J., Hannah, J.L., Coetzee, L.L., Beukes, N.J., 2004. Dating the rise of atmospheric oxygen. *Nature* **427**, 117–120.
- Bender, M., Sowers, T., Labeyrie, L., 1994. The Dole effect and its variations during the last 130,000 years as measured in the Vostok ice core. *Global Biogeochem. Cycles* **8**, 363–376.
- Berner, R.A., 2001. Modeling atmospheric O₂ over Phanerozoic time. *Geochim. Cosmochim. Acta* **65**, 685–694.
- Berner, R.A., 2005. The carbon and sulfur cycles and atmospheric oxygen from middle Permian to middle Triassic. *Geochim. Cosmochim. Acta* **69**, 3211–3217.
- Berner, R.A., Canfield, D.E., 1989. A new model for atmospheric oxygen over Phanerozoic time. *Am. J. Sci.* **289**, 333–361.
- Berner, R.A., Lasaga, A.C., Garrels, R.M., 1983. The carbonate-silicate geochemical cycle and its effect on atmospheric carbon dioxide over the past 100 million years. *Am. J. Sci.* **283**, 641–683.
- Blunier, T., Barnett, B., Bender, M.L., Hendricks, M.B., 2002. Biological oxygen productivity during the last 60,000 years from triple oxygen isotope measurements. *Global Biogeochem. Cycles* **16**, 15.
- Brenninkmeijer, C.A., Janssen, C., Kaiser, J., Rockmann, T., Rhee, T.S., Assonov, S.S., 2003. Isotope effects in the chemistry of atmospheric trace compounds. *Chem. Rev.* **103**, 5125–5162.
- Canfield, D.E., Teske, A., 1996. Late Proterozoic rise in atmospheric oxygen concentration inferred from phylogenetic and sulphur-isotope studies. *Nature* **382**, 127–132.
- Claypool, G.E., Holser, W.T., Kaplan, I.R., Sakai, H., Zak, I., 1980. The age curves of sulfur and oxygen isotopes in marine sulfate and their mutual interpretation. *Chem. Geol.* **28**, 199–260.
- Clayton, R.N., Grossman, L., Mayeda, T.K., 1973. A component of primitive nuclear composition in carbonaceous meteorites. *Science* **182**, 485–488.
- Cooper, G.W., Thiemens, M.H., Jackson, T.L., Chang, S., 1997. Sulfur and hydrogen isotope anomalies in meteorite sulfonic acids. *Science* **277**, 1072–1074.
- Craig, H., 1968. Isotope separation by carrier diffusion. *Science* **159**, 93–96.
- Craig, H., Horibe, Y., Sowers, T., 1988. Gravitational separation of gases and isotopes in polar ice caps. *Science* **242**, 1675–1678.
- Deines, P., 2003. A note on intra-elemental isotope effects and the interpretation of non-mass-dependent isotope variations. *Chem. Geol.* **199**, 179–182.
- Ding, T., Valkiers, S., Kipphardt, H., de Bievre, P., Taylor, P.D.P., Gonfiantini, R., Krouse, R., 2001. Calibrated sulfur isotope abundance ratios of three IAEA sulfur isotope reference materials and V-CDT with a reassessment of the atomic weight of sulfur. *Geochim. Cosmochim. Acta* **65**, 2433–2437.
- Farquhar, J., Wing, B.A., McKeegan, K.D., Harris, J.W., Cartigny, P., Thiemens, M.H., 2002. Mass-independent sulfur of inclusions in diamond and sulfur recycling on early Earth. *Science* **298**, 2369–2372.
- Farquhar, J., Bao, H., Thiemens, M., 2000a. Atmospheric influence of Earth's earliest sulfur cycle. *Science* **289**, 756–759.
- Farquhar, J., Jackson, T.L., Thiemens, M.H., 2000b. A S-33 enrichment in ureilite meteorites: evidence for a nebular sulfur component. *Geochim. Cosmochim. Acta* **64**, 1819–1825.
- Farquhar, J., Savarino, J., Jackson, T.L., Thiemens, M.H., 2000c. Evidence of atmospheric sulphur in the martian regolith from sulphur isotopes in meteorites. *Nature* **404**, 50–52.
- Farquhar, J., Johnston, D.T., Wing, B.A., Habicht, K.S., Canfield, D.E., Airieau, S., Thiemens, M.H., 2003. Multiple sulphur isotopic interpretations of biosynthetic pathways; implications for biological signatures in the sulphur isotope record. *Geobiology* **1**, 27–36.
- Gao, X., Thiemens, M.H., 1991. Systematic study of sulfur isotopic composition in iron meteorites and the occurrence of excess ³³S and ³⁶S. *Geochim. Cosmochim. Acta* **55**, 2671–2679.
- Gao, X., Thiemens, M.H., 1993a. Isotopic composition and concentration of sulfur in carbonaceous chondrites. *Geochim. Cosmochim. Acta* **57**, 3159–3169.
- Gao, X., Thiemens, M.H., 1993b. Variations of the isotopic composition of sulfur in enstatite and ordinary chondrites. *Geochim. Cosmochim. Acta* **57**, 3171–3176.
- Gao, Y.Q., Marcus, R.A., 2001. Strange and unconventional isotope effects in ozone formation. *Science* **293**, 259–263.
- Garrels, R.M., Lerman, A., 1981. Phanerozoic cycles of sedimentary carbon and sulfur. *Proc. Natl. Acad. Sci. USA* **78**, 4652–4656.
- Greenwood, J.P., Mojzsis, S.J., Coath, C.D., 2000. Sulfur isotopic compositions of individual sulfides in Martian meteorites ALH84001 and Nakhla; implications for crust-regolith exchange on Mars. *Earth Planet. Sci. Lett.* **184**, 23–35.
- Hoering, T.C., 1989. Development of the sulfur hexafluoride method for sulfur isotope analysis. *Annual Report of the Director, Geophysical Laboratory, Carnegie Institution, Report: 2200*, 128–131.
- Holser, W.T., Kaplan, I.R., 1966. Isotope geochemistry of sedimentary sulfates. *Chem. Geol.* **1**, 93–135.
- Holser, W.T., Maynard, J.B., Cruikshank, K.M., 1989. Modeling the natural cycle of sulphur through Phanerozoic time. In: Brimblecombe, P., Lein, A.Y. (Eds.), *Evolution of the Global Biogeochemical Sulphur Cycle*. Wiley, New York, pp. 21–56.
- Hu, G.X., Rumble, D., Wang, P.L., 2003. An ultraviolet laser microprobe for the in situ analysis of multisulfur isotopes and its use in measuring Archean sulfur isotope mass-independent anomalies. *Geochim. Cosmochim. Acta* **67**, 3101–3118.
- Hulston, J.R., Thode, H.G., 1965a. Cosmic-ray-produced S³⁶ and S³³ in the metallic phase of iron meteorites. *J. Geophys. Res.* **70**, 4435–4442.
- Hulston, J.R., Thode, H.G., 1965b. Variations in the S³³, S³⁴, and S³⁶ contents of meteorites and their relation to chemical and nuclear effects. *J. Geophys. Res.* **70**, 3475–3484.
- Jensen, M.L., Nakai, N., 1962. Sulfur isotope meteorite standards; results and recommendations. In: Jensen, M.L. (Ed.), *Biogeochemistry of Sulfur Isotopes. NSF Symposium*, pp. 30–35.
- Johnston, D.T., Farquhar, J., Wing, B., Kaufman, A.J., Canfield, D.E., Habicht, K.S., 2005. Multiple sulfur fractionations in biological systems: a case study with sulfate reducers and sulfur disproportionators. *Am. J. Sci.* **305**, 645–660.
- Kaiser, J., Rockmann, T., Brenninkmeijer, C.A.M., 2004. Contribution of mass-dependent fractionation to the oxygen isotope anomaly of atmospheric nitrous oxide – art. no. D03305. *J. Geophys. Res.* **109**. doi:10.1029/2003JD004088.
- Kaplan, I.R., Rittenberg, S.C., 1964. Microbiological fractionation of sulphur isotopes. *J. Gen. Microbiol.* **34**, 195–212.
- Luz, B., Barkan, E., 2000. Assessment of oceanic productivity with the triple-isotope composition of dissolved oxygen. *Science* **288**, 2028–2031.
- Luz, B., Barkan, E., 2005. The isotopic ratios ¹⁷O/¹⁶O and ¹⁸O/¹⁶O in molecular oxygen and their significance in biochemistry. *Geochim. Cosmochim. Acta* **69**, 1099–1110.
- Luz, B., Barkan, E., Bender, M.L., Thiemens, M.H., Boering, K.A., 1999. Triple-isotope composition of atmospheric oxygen as a tracer of biosphere productivity. *Nature* **400**, 547–550.

- Mariotti, A., Germon, J.C., Hubert, P., Kaiser, P., Letolle, R., Tardieux, A., Tardieux, P., 1981. Experimental determination of nitrogen kinetic isotope fractionation: some principles; illustration for the denitrification and nitrification processes. *Plant Soil* **62**, 413–430.
- Mauersberger, K., Erbacher, B., Krankowsky, D., Günther, J., Nickel, R., 1999. Ozone isotope enrichment: isotopomer-specific rate coefficients. *Science* **283**, 370–372.
- Meijer, H.A.J., Li, W.J., 1998. The use of electrolysis for accurate $\delta^{17}\text{O}$ and $\delta^{18}\text{O}$ isotope measurements in water. *Isotopes Environ. Health Stud.* **34**, 349–369.
- Miller, M.F., 2002. Isotopic fractionation and the quantification of ^{17}O anomalies in the oxygen three-isotope system; an appraisal and geochemical significance. *Geochim. Cosmochim. Acta* **66**, 1881–1889.
- Miller, M.F., Franchi, I.A., Pillinger, C.T., Anonymous, 1999. High precision measurements of the oxygen isotope mass-dependent fractionation line for the Earth–Moon system. *Proc. Goldschmidt IX*, 7433.
- Mojzsis, S.J., Coath, C.D., Greenwood, J.P., McKeegan, K.D., Harrison, T.M., 2003. Mass-independent isotope effects in Archean (2.5–3.8 Ga) sedimentary sulfides determined by ion microprobe analysis. *Geochim. Cosmochim. Acta* **67**, 1635–1658.
- Northrop, D.B., 1975. Steady-state analysis of kinetic isotope effects in enzymic reactions. *Biochemistry* **14**, 2644–2651.
- Ohmoto, H., 1992. Biogeochemistry of sulfur and the mechanisms of sulfide-sulfate mineralization in Archean oceans. In: Schidlowski, M. (Ed.), *Early Organic Evolution: Implications for Mineral and Energy Resources*. Springer, Berlin, pp. 378–397.
- Ohmoto, H., Goldhaber, M.B., 1997. Sulfur and carbon isotopes. In: Barnes, H.L. (Ed.), *Geochemistry of Hydrothermal Ore Deposits*. Wiley, New York.
- Oliver, N.H., Hoering, T.C., Johnston, T.W., Rumble, D., Shanks III, W.C., 1992. Sulfur isotopic disequilibrium and fluid–rock interaction during metamorphism of sulfidic black shales from the Waterville-Augusta area, Maine, USA. *Geochim. Cosmochim. Acta* **56**, 4257–4265.
- Ono, S., Eigenbrode, J.L., Pavlov, A.A., Kharecha, P., Rumble, D., Kasting, J.F., Freeman, K.H., 2003. New insights into Archean sulfur cycle from mass-independent sulfur isotope records from the Hamersley Basin, Australia. *Earth Planet. Sci. Lett.* **213**, 15–30.
- Pavlov, A.A., Kasting, J.F., 2002. Mass-independent fractionation of sulfur isotopes in Archean sediments: strong evidence for an anoxic Archean atmosphere. *Astrobiology* **2**, 27–41.
- Rees, C.E., 1973. A steady-state model for sulphur isotope fractionation in bacterial reduction processes. *Geochim. Cosmochim. Acta* **37**, 1141–1162.
- Rees, C.E., Thode, H.G., 1974. Sulphur concentrations and isotope ratios in Apollo 16 and 17 samples. *Lunar Science V* (Part 2), 621–623.
- Robinson, B.W., 1993. Sulphur isotope standard. In: *Reference and Intercomparison Materials for Stable Isotopes of Light Elements*, vol. IAEA-TECHDOC-825, pp. 39–45. IAEA.
- Rumble, D., Hoering, T.C., Palin, J.M., 1993. Preparation of SF_6 for sulfur isotope analysis by laser heating sulfide minerals in the presence of F_2 gas. *Geochim. Cosmochim. Acta* **57**, 4499–4512.
- Rumble III, D., Oliver, N.H.S., Ferry, J.M., Hoering, T.C., 1991. Carbon and oxygen isotope geochemistry of chlorite-zone rocks of the Waterville Limestone, Maine, USA. *Am. Mineralogist* **76**, 857–866.
- Schueler, B., Morton, J., Mauersberger, K., 1990. Measurement of isotopic abundances in collected stratospheric ozone samples. *Geophys. Res. Lett.* **17**, 1295–1298.
- Sessions, A.L., Hayes, J.M., 2005. Calculation of hydrogen isotopic fractionations in biogeochemical systems. *Geochim. Cosmochim. Acta* **69**, 593–597.
- Skaron, S., Wolfsberg, M., 1980. Anomalies in the fractionation by chemical equilibrium of $^{18}\text{O}/^{16}\text{O}$ relative to $^{17}\text{O}/^{16}\text{O}$. *J. Chem. Phys.* **72**, 6810–6811.
- Stewart, G.A., 1927. Fauna of the Silica Shale of Lucas County. *Ohio Geological Survey Bulletin* **32**, 76.
- Strauss, H., 1997. The isotopic composition of sedimentary sulfur through time. *Palaeogeogr. Palaeoclimatol. Palaeoecol.* **132**, 97–118.
- Thiemens, M.H., 1999. Mass-independent isotope effects in planetary atmospheres and the early solar system. *Science* **283**, 341–345.
- Thiemens, M.H., Heidenreich III, J.E., 1983. The mass-independent fractionation of oxygen; a novel isotope effect and its possible cosmochemical implications. *Science* **219**, 1073–1075.
- Thode, H.G., Rees, C.E., 1971. Measurement of sulphur concentrations and the isotope ratios $^{33}\text{S}/^{32}\text{S}$, $^{34}\text{S}/^{32}\text{S}$ and $^{36}\text{S}/^{33}\text{S}$ in Apollo 12 samples. *Earth Planet. Sci. Lett.* **12**, 434–438.
- Wing, B.A., Brabson, E., Farquhar, J., Kaufman, A.J., Rumble, D., Bekker, A., 2002. $\Delta^{33}\text{S}$, $\delta^{34}\text{S}$ and $\delta^{13}\text{C}$ constraints on the Paleoproterozoic atmosphere during the earliest Huronian glaciation. In: *12th Goldschmidt Conference*, A840.
- Young, E.D., Galy, A., Nagahara, H., 2002. Kinetic and equilibrium mass-dependent isotope fractionation laws in nature and their geochemical and cosmochemical significance. *Geochim. Cosmochim. Acta* **66**, 1095–1104.